# STRUCTURE OF GALAXIES

## Lecture 4. Observations of kinematics; dynamical relations and distance determinations.

HI observations of spiral galaxies.

As an example I take the observations of NGC 3198 with the Westerbork Synthesis Radio Telescope. These observations are part of the Palomar-Westerbork Survey of northern spiral galaxies*.

This survey combined 21-cm observations of the neutral hydrogen with three-color optical surface photometry from photographic plates with the Palomar 48-inch Schmidt-telescope.

HI observations are done in narrow frequency channels with widths of order ten or a few tens of km/s. The first thing to do is add up the channels at which no HI is present to find the continuum map.

*Wevers, Ph.D. Thesis, 1984, Wevers, van der Kruit & Allen, A.&A.Suppl. 66, 505 (1986)

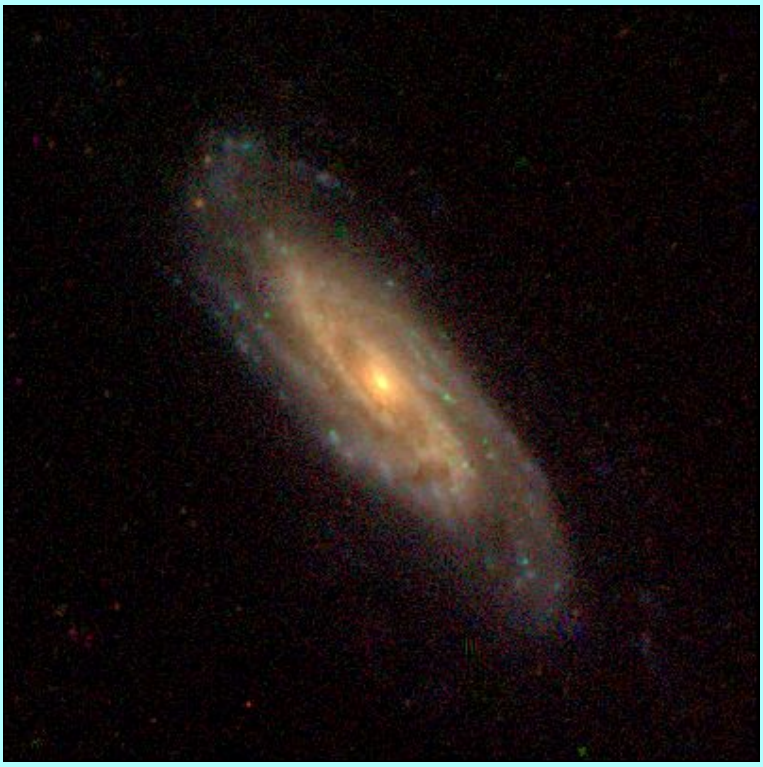

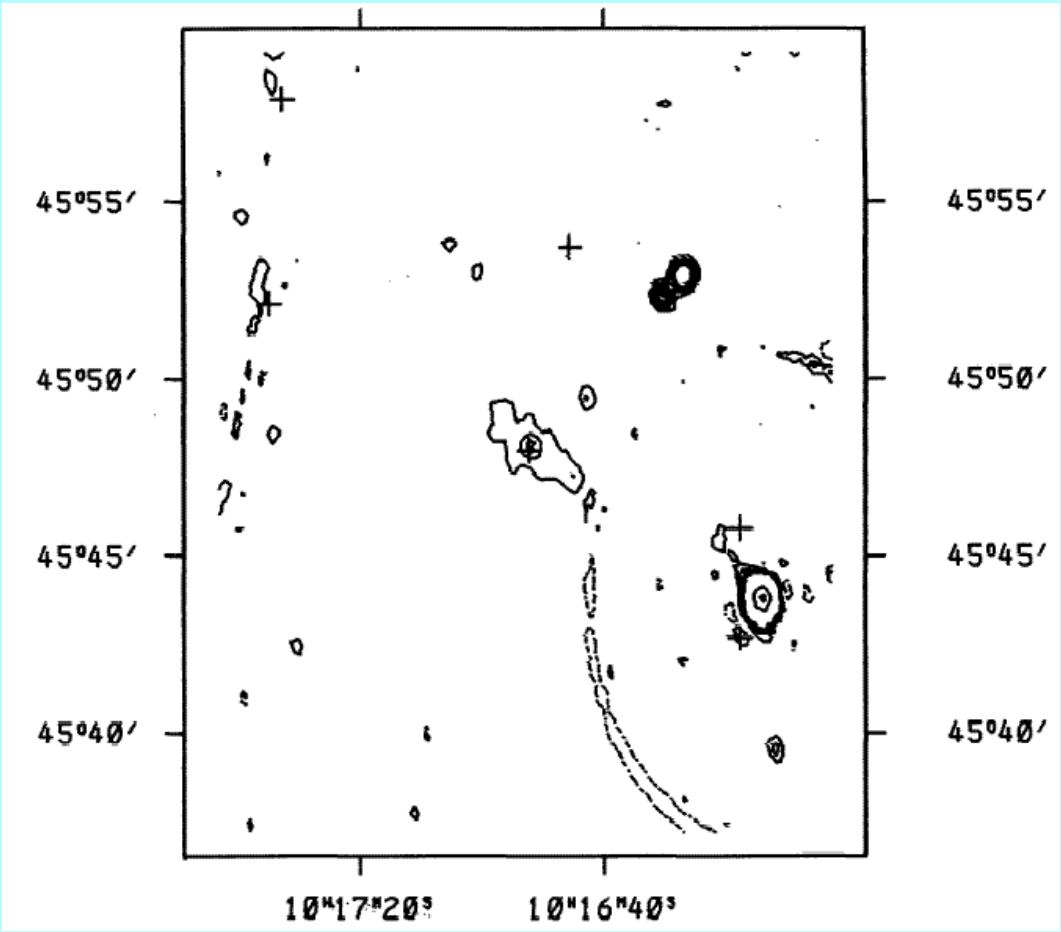
45°55′
45°50′
45°45′
45°40′
10ʰ17ᵐ20ˢ
10ʰ16ᵐ40ˢ

The continuum radiation is mostly non-thermal synchrotron emission from relativistic electrons moving in the galactic magnetic field.

At the position of the HII-regions there also is thermal free-free emission from interaction between free electrons and ionized hydrogen (protons).

This particular galaxy has radio emission from the center and some extended faint emission from the disk.

This continuum map is then subtracted from all channel maps to reveal the distribution of HI at various velocities.

The continuum map should be produced from as many channel maps as possible, so that the noise in it is low compared to that in the channel maps themselves.

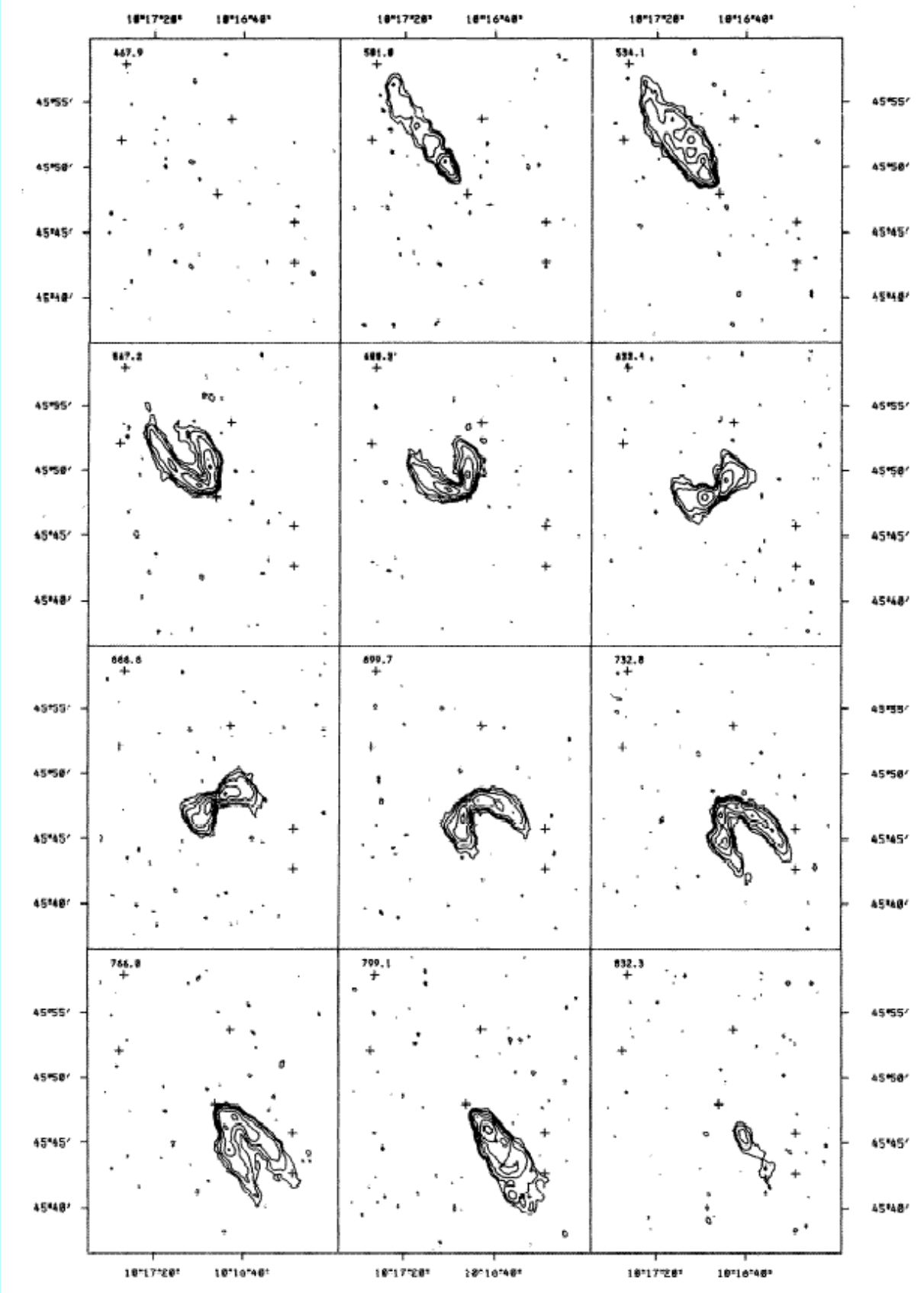
18°17'20"
18°16'40"
45°55'
45°50'
45°45'
45°40'
467.9
581.8
534.1
647.2
688.8
633.4
666.6
699.7
732.8
766.8
799.1
832.3

These channel maps can be added to produce the map with the distribution of neutral hydrogen, the total HI-map.

To suppress noise usually this is preceded by blocking out the areas in each of the channel maps that appear to have no HI-signal and thus contain only noise.

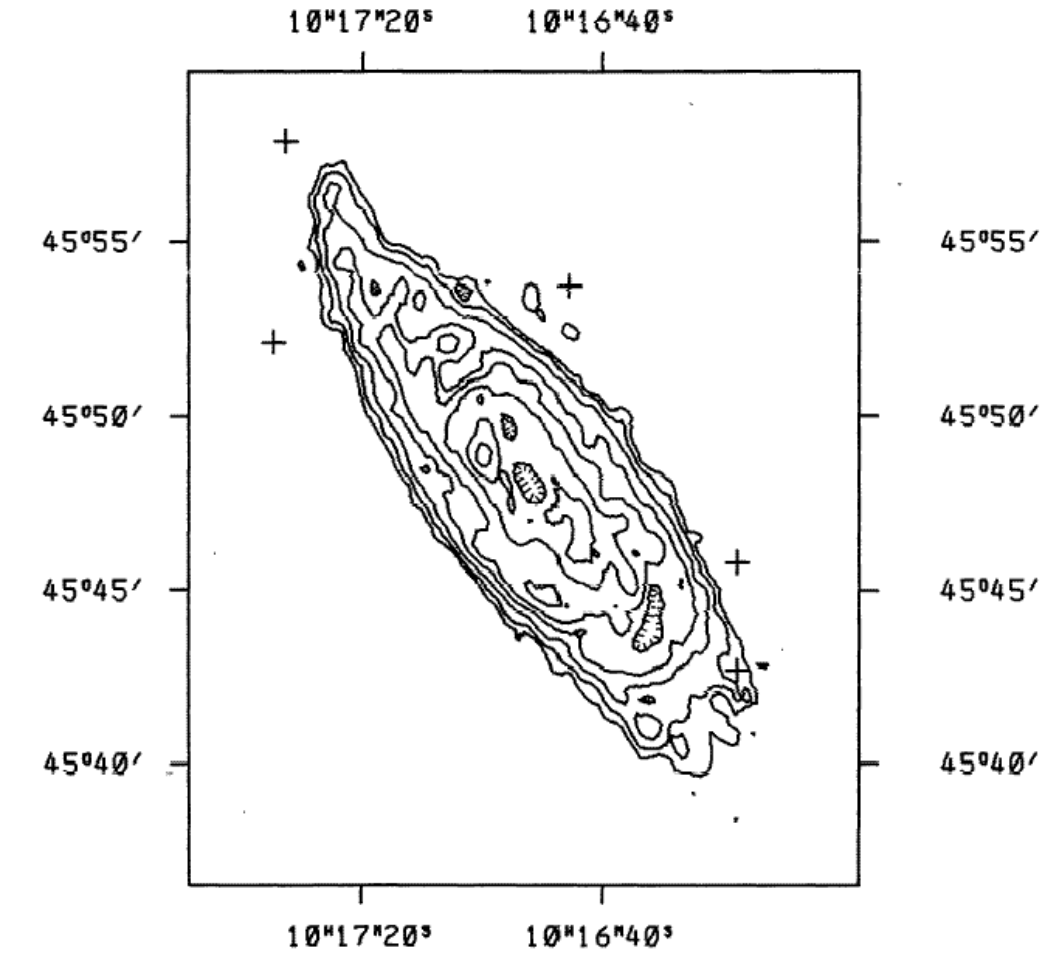

From this map the radial HI profile can be produced by averaging in azimuthal annuli.

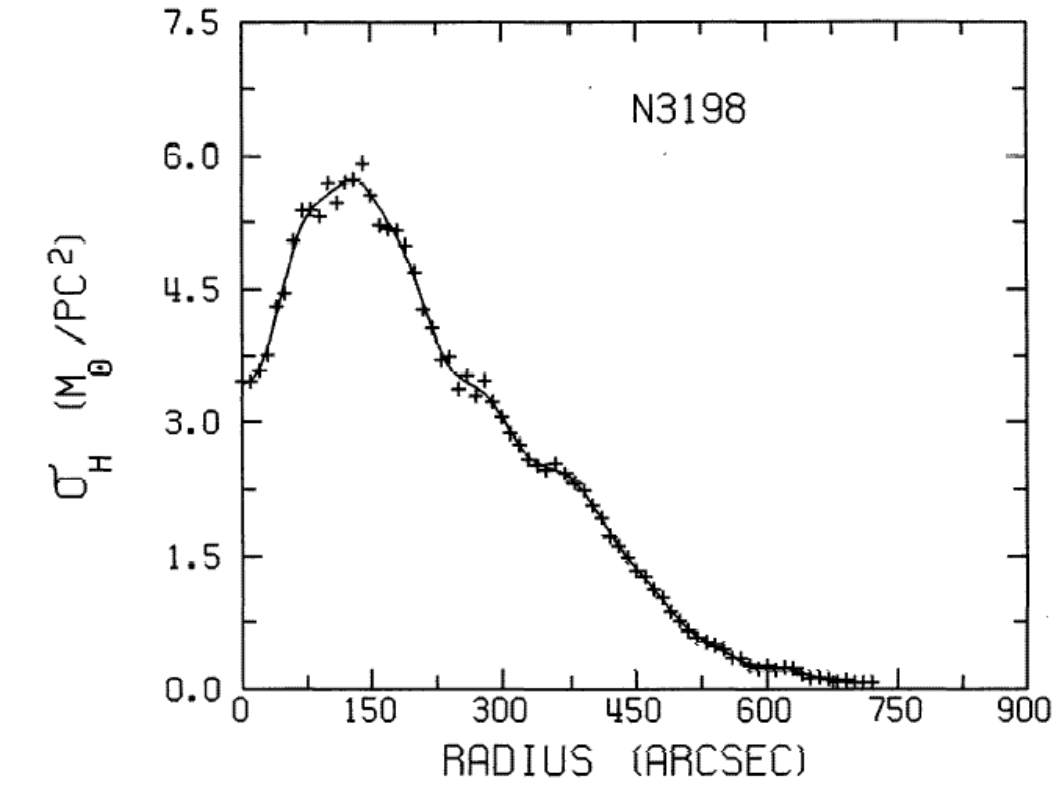


In practice this is done after analysis of the velocity field in order to find the position of the center and the orientation parameters (direction of major axis and inclination).

One can then take the optical map(s) and derive the radial luminosity profiles.

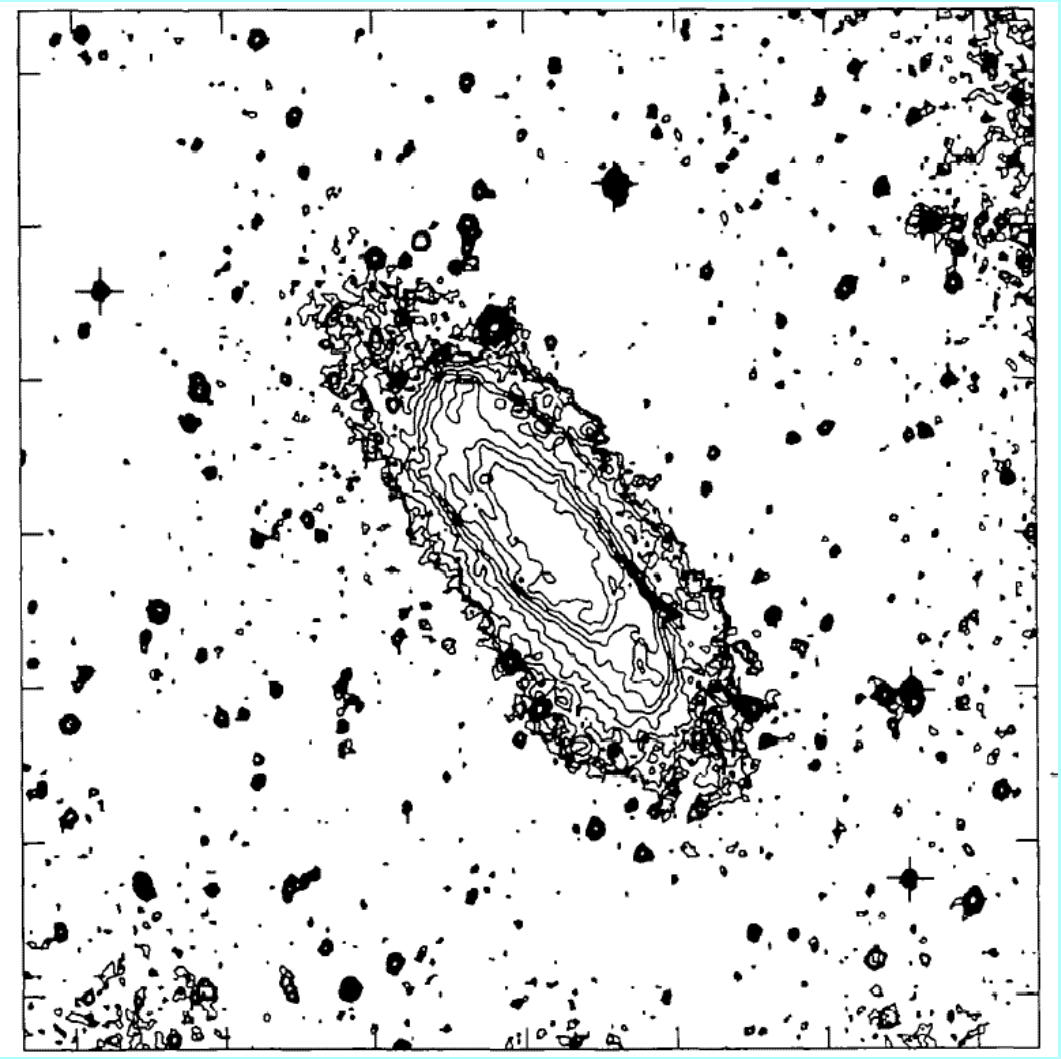

These can be further extended with radial color profiles and radial profile of the HI-surface density versus optical surface luminosity.

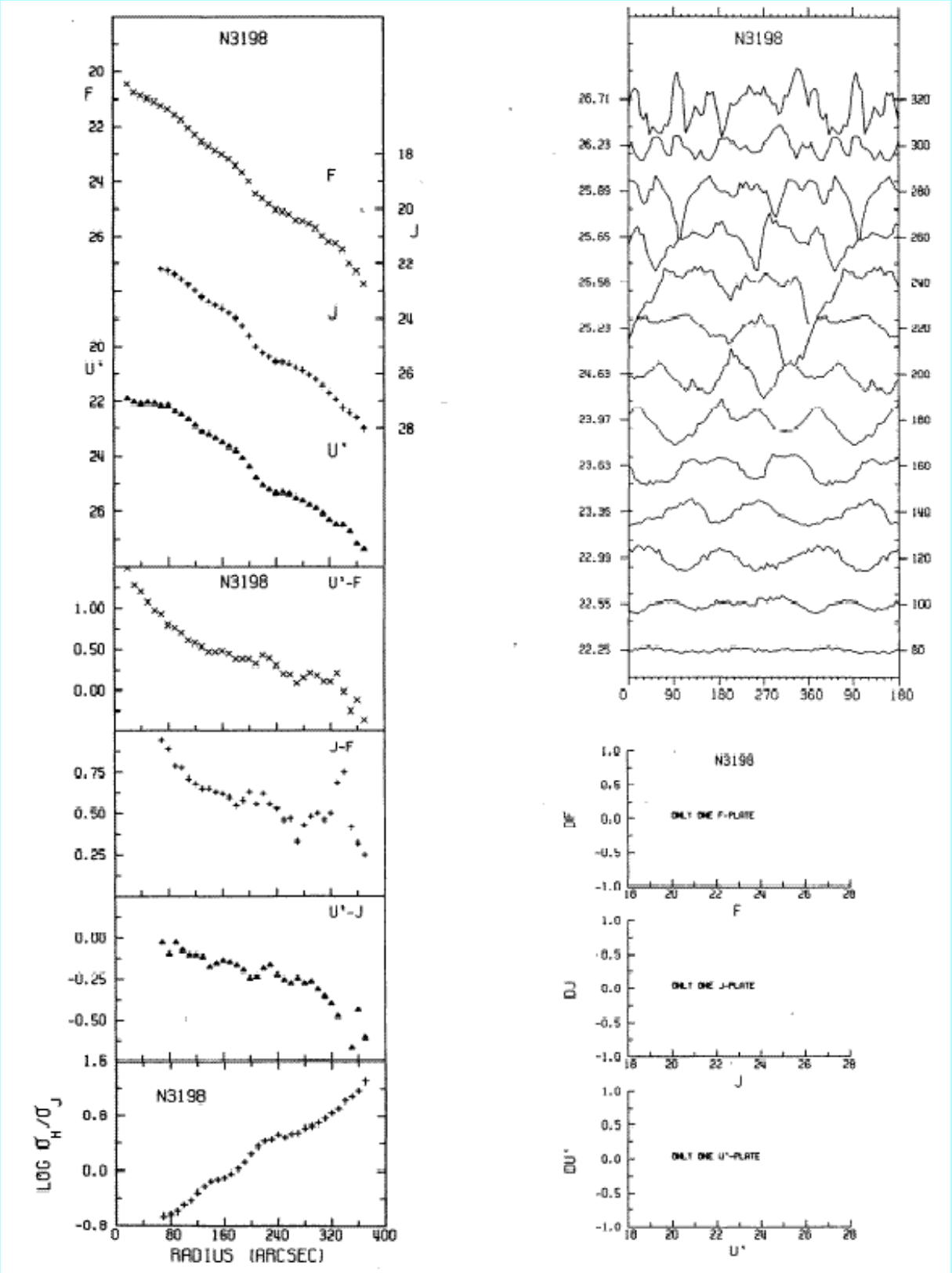
N3198
F
J
U'
U'-F
J-F
U'-J
N3198
LOG σ_H/σ_J
RADIUS (ARCSEC)
N3198
ONLY ONE F-PLATE
ONLY ONE J-PLATE
ONLY ONE U'-PLATE
ΔF
ΔJ
ΔU'

The profiles are tabulated below.

The units are magnitudes per arcsec$^2$ for surface brightness (which can be translated in solar luminosities per pc$^2$), magnitudes for color, solar masses per pc$^2$ for HI-surface densities and solar masses over solar luminosities for the density brightness ratio.

NGC 3198 surface brightness

| radius arcsec | U' | J | F | U'-J | J-F | U'-F |
|---|---|---|---|---|---|---|
| 0. | - | - | - | - | - | - |
| 10. | - | - | - | - | - | - |
| 20. | 21.91 | - | 20.43 | - | - | 1.48 |
| 30. | 22.03 | - | 20.75 | - | - | 1.28 |
| 40. | 22.08 | - | 20.88 | - | - | 1.20 |
| 50. | 22.04 | - | 20.97 | - | - | 1.07 |
| 60. | 22.07 | - | 21.10 | - | - | 0.97 |
| 70. | 22.16 | 22.19 | 21.24 | -0.03 | 0.95 | 0.92 |
| 80. | 22.15 | 22.25 | 21.36 | -0.10 | 0.89 | 0.79 |
| 90. | 22.35 | 22.38 | 21.59 | -0.03 | 0.79 | 0.76 |
| 100. | 22.46 | 22.54 | 21.76 | -0.08 | 0.78 | 0.70 |
| 110. | 22.65 | 22.76 | 22.05 | -0.11 | 0.71 | 0.60 |
| 120. | 22.88 | 22.99 | 22.31 | -0.11 | 0.68 | 0.57 |
| 130. | 23.08 | 23.20 | 22.55 | -0.12 | 0.65 | 0.53 |
| 140. | 23.18 | 23.36 | 22.71 | -0.18 | 0.65 | 0.47 |
| 150. | 23.33 | 23.49 | 22.86 | -0.16 | 0.63 | 0.47 |
| 160. | 23.49 | 23.63 | 23.01 | -0.14 | 0.62 | 0.48 |
| 170. | 23.64 | 23.79 | 23.19 | -0.15 | 0.60 | 0.45 |
| 180. | 23.80 | 23.97 | 23.42 | -0.17 | 0.55 | 0.38 |
| 190. | 24.05 | 24.25 | 23.67 | -0.20 | 0.58 | 0.38 |
| 200. | 24.39 | 24.64 | 24.01 | -0.25 | 0.63 | 0.38 |
| 210. | 24.76 | 25.00 | 24.44 | -0.24 | 0.56 | 0.32 |
| 220. | 25.05 | 25.24 | 24.62 | -0.19 | 0.62 | 0.43 |
| 230. | 25.22 | 25.39 | 24.83 | -0.17 | 0.56 | 0.39 |
| 240. | 25.33 | 25.56 | 25.03 | -0.23 | 0.53 | 0.30 |
| 250. | 25.31 | 25.57 | 25.11 | -0.26 | 0.46 | 0.20 |
| 260. | 25.37 | 25.65 | 25.18 | -0.28 | 0.47 | 0.19 |
| 270. | 25.51 | 25.76 | 25.43 | -0.25 | 0.33 | 0.08 |
| 280. | 25.60 | 25.88 | 25.45 | -0.28 | 0.43 | 0.15 |
| 290. | 25.77 | 26.04 | 25.56 | -0.27 | 0.48 | 0.21 |
| 300. | 25.89 | 26.21 | 25.71 | -0.32 | 0.50 | 0.18 |
| 310. | 26.08 | 26.44 | 25.98 | -0.36 | 0.46 | 0.10 |
| 320. | 26.30 | 26.70 | 26.20 | -0.40 | 0.50 | 0.10 |
| 330. | 26.46 | 26.94 | 26.25 | -0.48 | 0.69 | 0.21 |
| 340. | 26.47 | 27.24 | 26.49 | -0.77 | 0.75 | -0.02 |
| 350. | 26.74 | 27.41 | 26.99 | -0.67 | 0.42 | -0.25 |
| 360. | 27.15 | 27.59 | 27.27 | -0.44 | 0.32 | -0.12 |
| 370. | 27.37 | 27.98 | 27.73 | -0.61 | 0.25 | -0.36 |

NGC 3198 HI surface density

| radius arcsec | $\sigma$(HI) $M_\odot/pc^2$ | $\sigma$(J) $L_\odot/pc^2$ | LOG($\sigma$(HI)/$\sigma$(J)) $M_\odot/L_\odot$ |
|---|---|---|---|
| 0. | 3.453 | - | - |
| 30. | 3.758 | - | - |
| 60. | 5.039 | - | - |
| 90. | 5.312 | 20.800 | -.593 |
| 120. | 5.706 | 11.859 | -.318 |
| 150. | 5.553 | 7.483 | -.129 |
| 180. | 5.154 | 4.809 | .030 |
| 210. | 4.262 | 5.862 | .360 |
| 240. | 3.741 | 1.112 | .527 |
| 270. | 3.299 | .925 | .552 |
| 300. | 3.057 | .611 | .699 |
| 330. | 2.586 | .312 | .919 |
| 360. | 2.546 | .171 | 1.172 |
| 390. | 2.238 | - | - |
| 420. | 1.723 | - | - |
| 450. | 1.331 | - | - |
| 480. | 1.024 | - | - |
| 510. | .656 | - | - |
| 540. | .499 | - | - |
| 570. | .355 | - | - |
| 600. | .271 | - | - |
| 630. | .236 | - | - |
| 660. | .132 | - | - |
| 690. | .105 | - | - |
| 720. | .081 | - | - |

The velocity field follows from deriving at each position the radial velocity.

This can be done either by moment analysis of the HI-profile or a fit with a Gaussian.

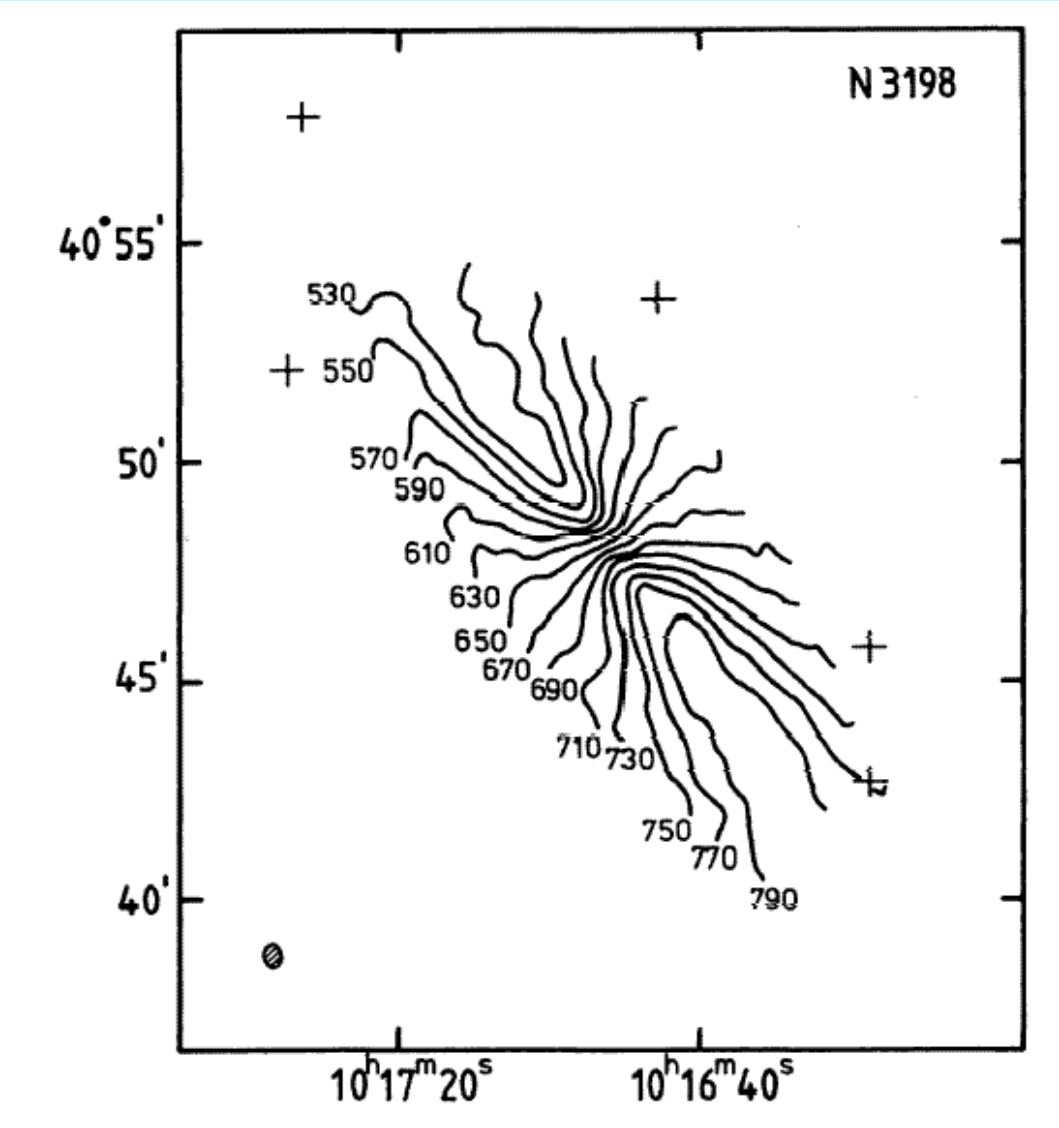


This is called a spider diagram.

Helpful for further analysis are also position-velocity diagrams (or x,V-diagrams), which have position along a line (or curve) on one axis and radial velocity on the other.

The following figure shows the x,V-diagrams along the major and minor axis.

Also useful is the integrated profile.

The next step is to analyse the velocity field in terms of the orientation of the plane of the disk and the rotation curve.

A first guess for the major axis direction and the inclination can be obtained from the distribution of HI and/or the optical image.

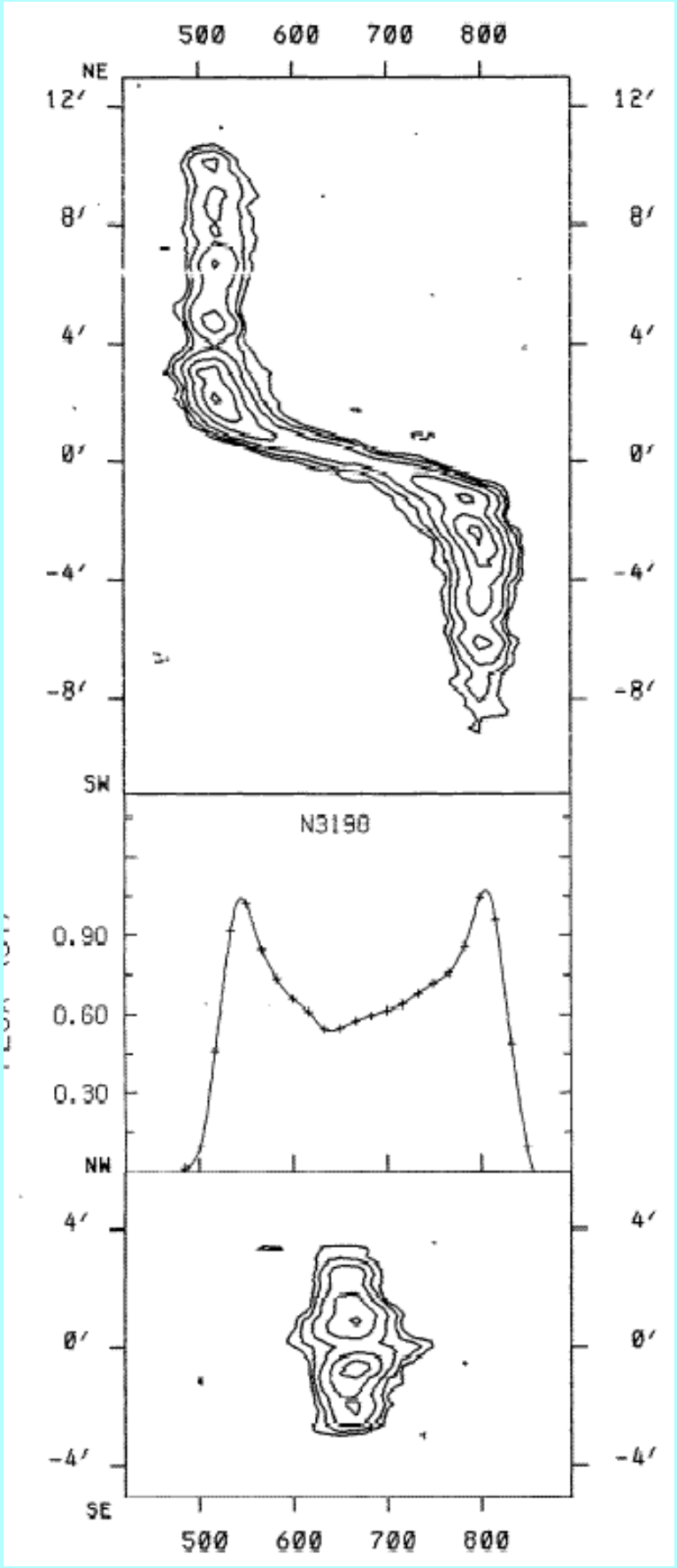
500
600
700
800
NE
12′
8′
4′
0′
-4′
-8′
SW
N3190
0.90
0.60
0.30
NW
SE

Assume we have a disk galaxy with a rotation curve $V_{\rm rot}(R)$. The position angle of the major axis is $\Phi_\circ$ and the inclination is $i$ (defined as zero for face-on).

Take the coordinates on the sky as $(r, \Phi)$ and in the plane of the galaxy $(R, \theta)$.

Then

$$R = r\frac{\cos(\Phi - \Phi_\circ)}{\cos\theta}$$

$$\tan\theta = \frac{\tan(\Phi - \Phi_\circ)}{\cos i}$$

$$V_{\rm obs} = V_{\rm sys} + V_{\rm rot}(R)\sin i\cos\theta$$

We can calculate the pattern of the residual velocity field after subtraction of a model. We then see that errors in each parameter produce different patterns and therefore in principle these parameters can be determined independently*.

*see van der Kruit & Allen, Ann.Rev.Astron.Astrophys. 16, 103 (1978)

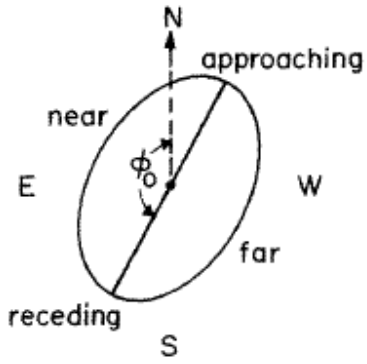


$V_{obs} = V_{sys} + V_\theta \sin i \cos\theta + V_R \sin i \sin\theta$

Sky $(r, \phi)$ $\quad tg\,\theta = tg(\phi - \phi_0)/\cos i$

Plane of galaxy $(R, \theta)$ $\quad R = r \cos(\phi - \phi_0)/\cos\theta$

$V_{observed} - V_{model}$


$V_{sys}$ too large

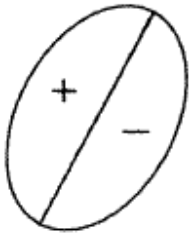


$\phi_0$ too large

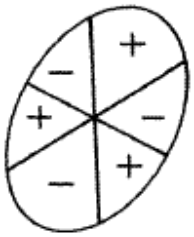


i too large

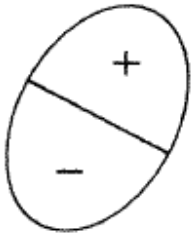


$V_{rot}$ too large

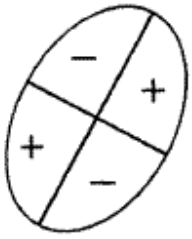


R.C. to east on minor axis

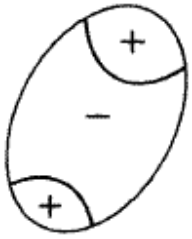


R.C. to north on major axis

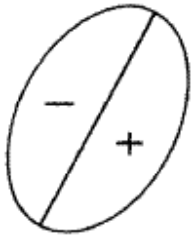


$V_R > 0$

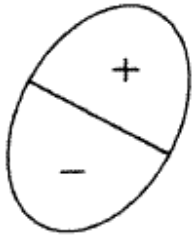


$V_\theta < V_{rot}$

The usual procedure to determine the velocity field is as follows.

From the optical maps the position of the center, the position angle of the major axis and the inclination are estimated.

Then in rings in the galaxy plane (which corresponds to ellipses on the sky) the observed velocities are converted into "rotation velocities" along the ring.

Then changes in the parameters are introduced; this changes the run of deduced rotation velocity along the ring.

The parameters are optimized until these variations along the ring are minimal.

In practice it turns out that in particular in the outer regions the planes of the rings change.

This is illustrated with the observations of NGC 5055*.

*Bosma, Ph.D. thesis, 1978; A.J. 86, 1791 (1981)

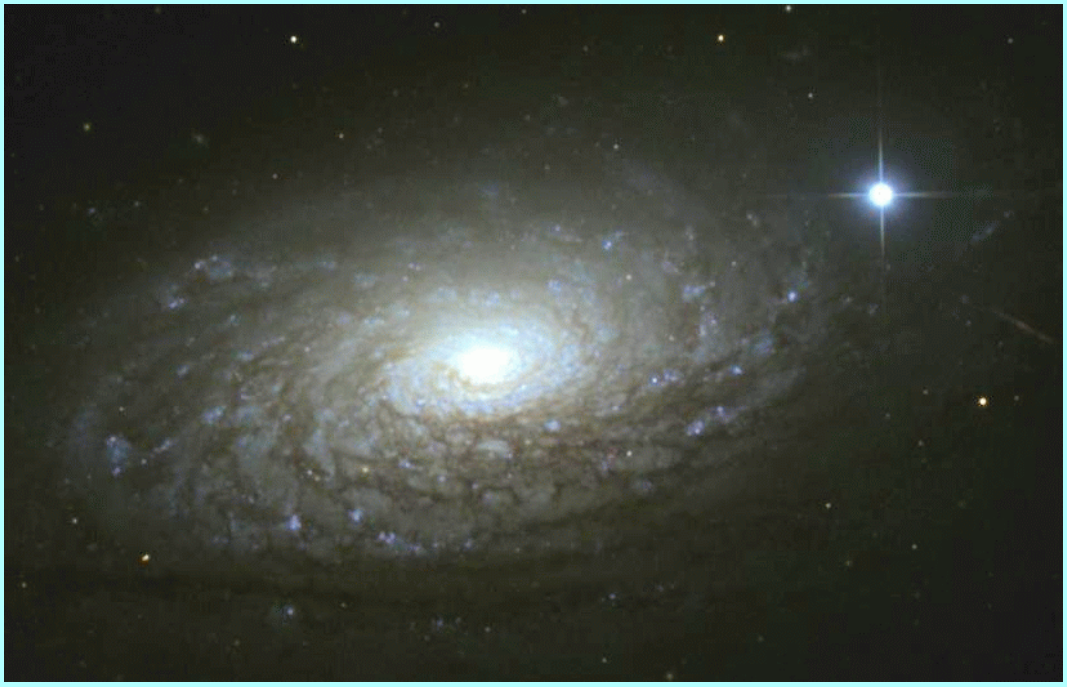

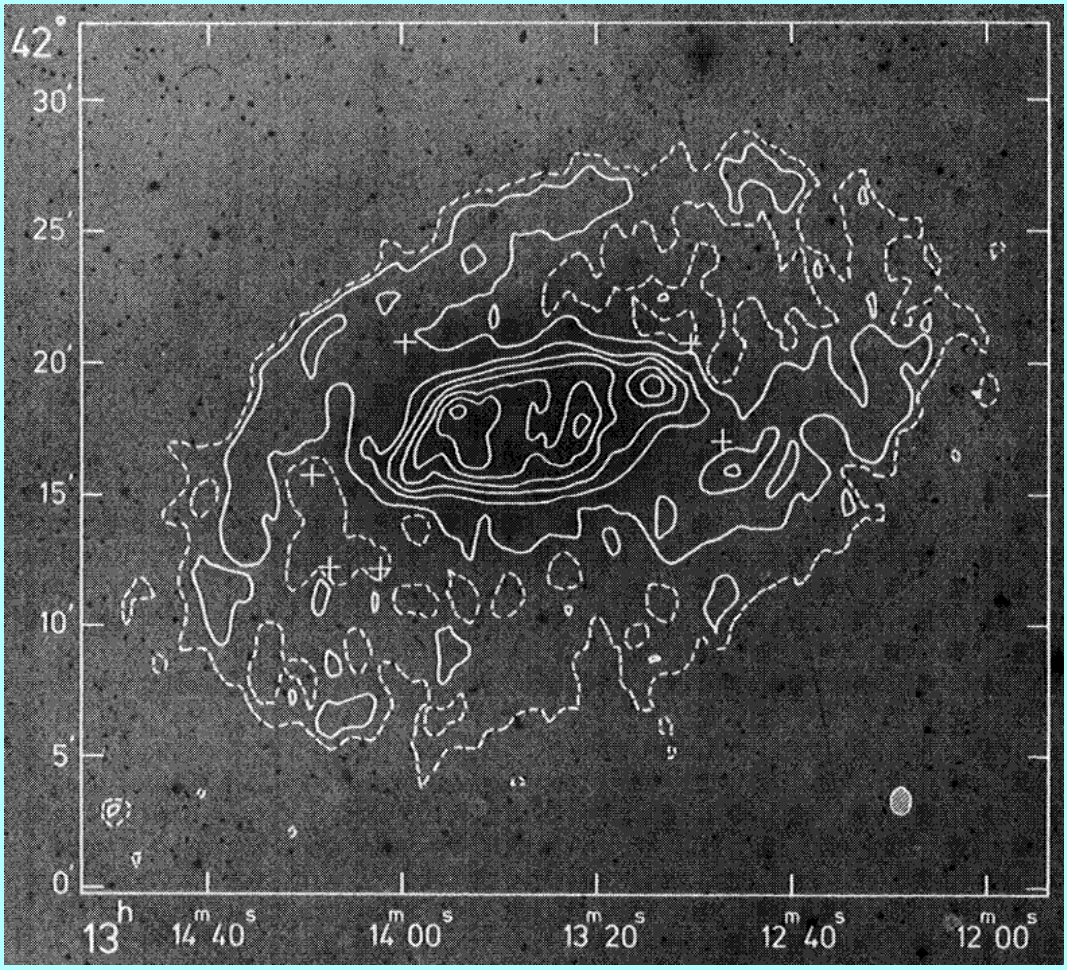
42°
30′
25′
20′
15′
10′
5′
0′
13h 14m 40s
14m 00s
13m 20s
12m 40s
12m 00s

The distribution of the HI in the outer parts suggests that the plane of the disk changes. This is called a "warp".

We also see distortions in the velocity field.

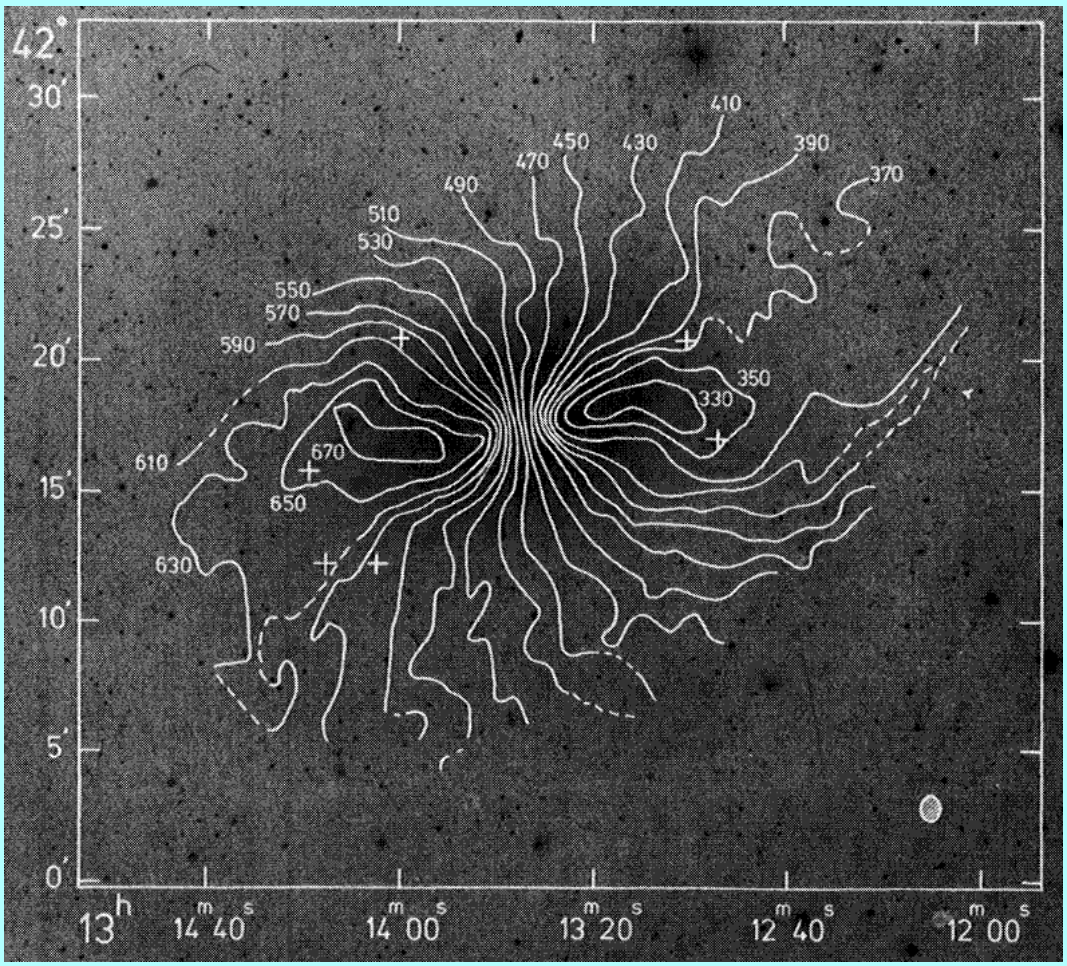


The distribution and velocity field of the HI can be fitted with "inclined rings".

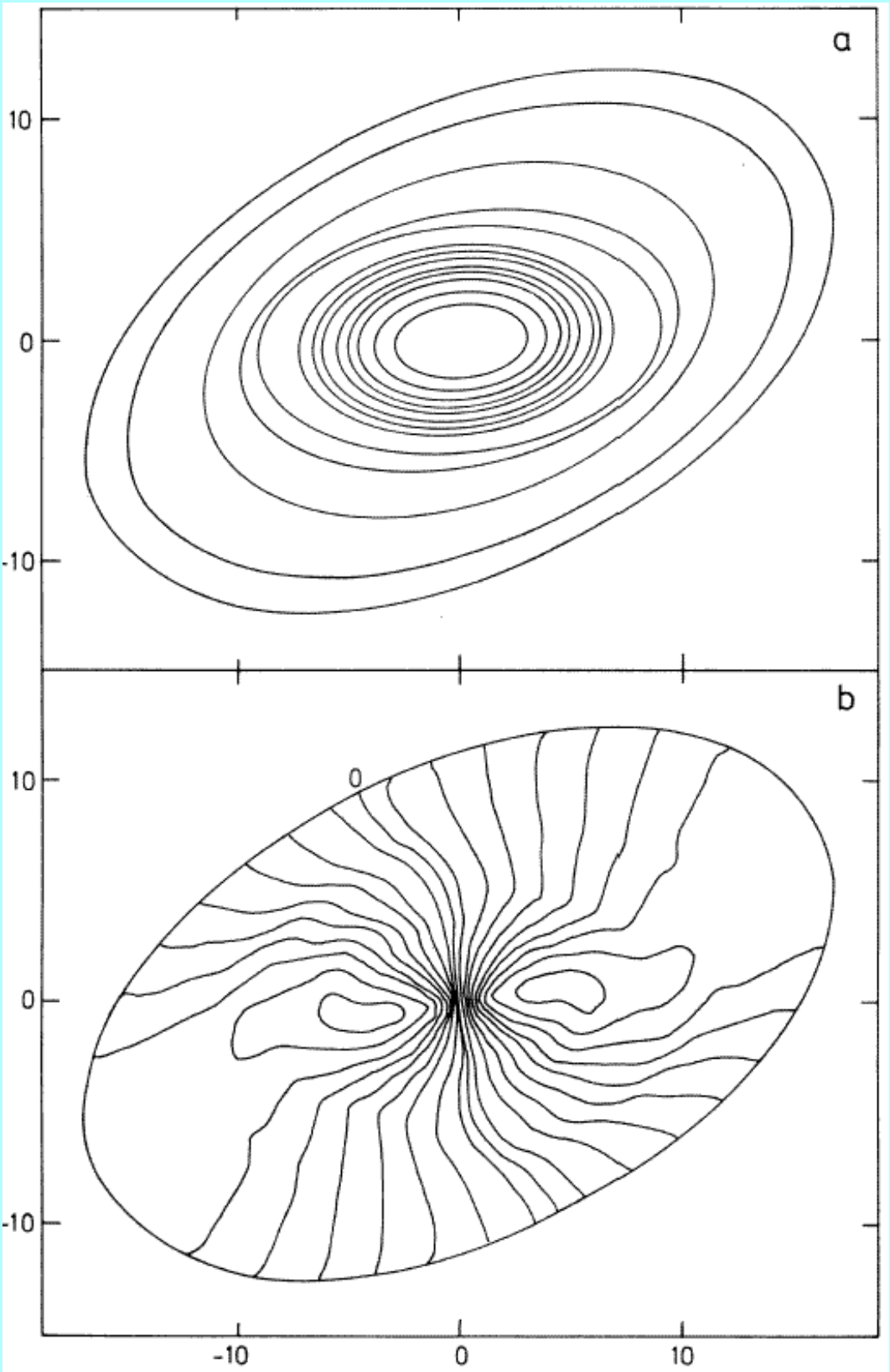
a
10
0
-10
b
10
0
-10
0
-10
0
10

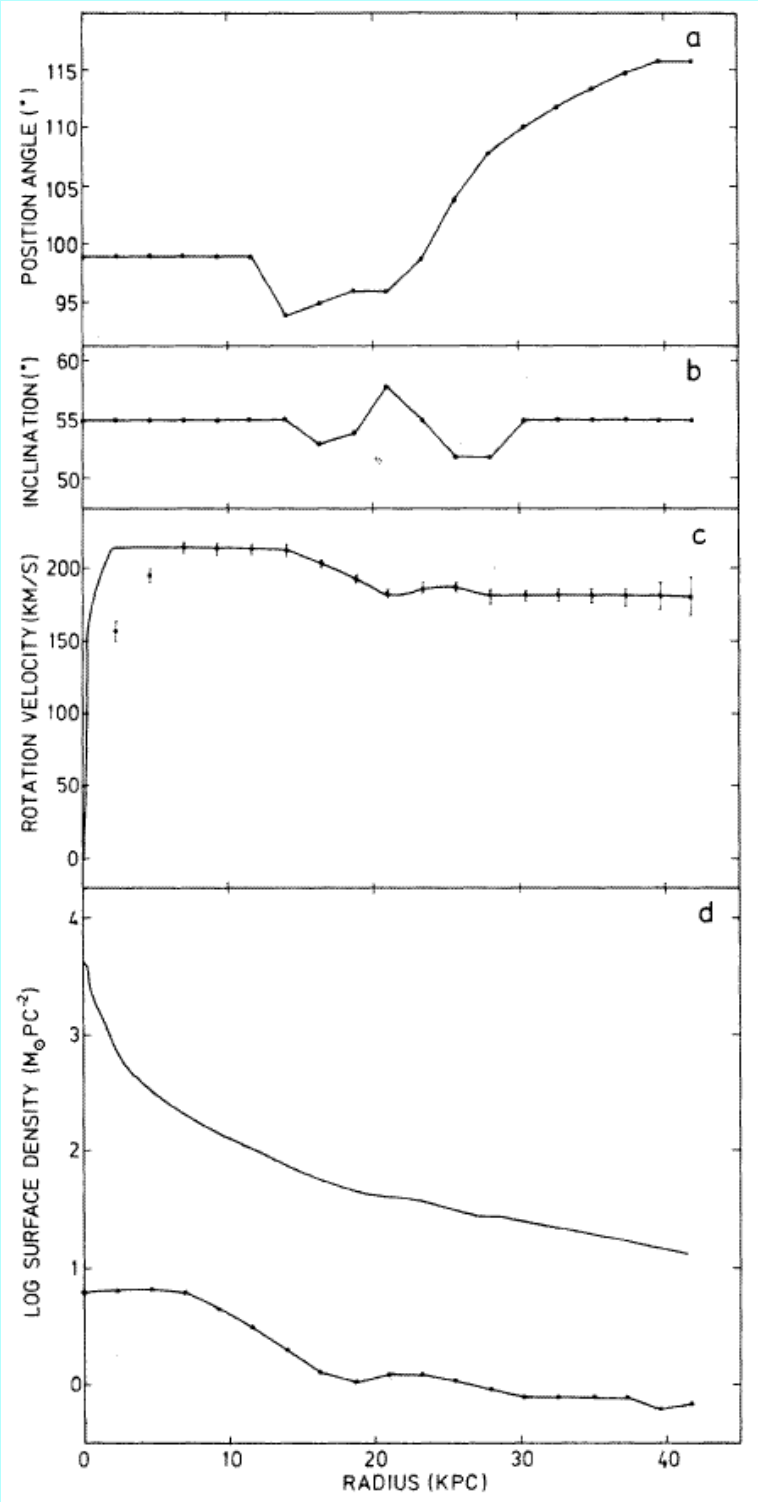
a
POSITION ANGLE (°)
115
110
105
100
95
b
INCLINATION (°)
60
55
50
c
ROTATION VELOCITY (KM/S)
200
150
100
50
0
d
LOG SURFACE DENSITY ($M_\odot PC^{-2}$)
4
3
2
1
0
0
10
20
30
40
RADIUS (KPC)

The warps in the HI appear to start usually at the edges of the optical (stellar) disk.

Another example is NGC 628. This is close to face-on and can therefore be used to measure the velocity dispersion of the HI.

The fact the NGC 628 is close to face-on is visible in the width of the integrated HI profile.

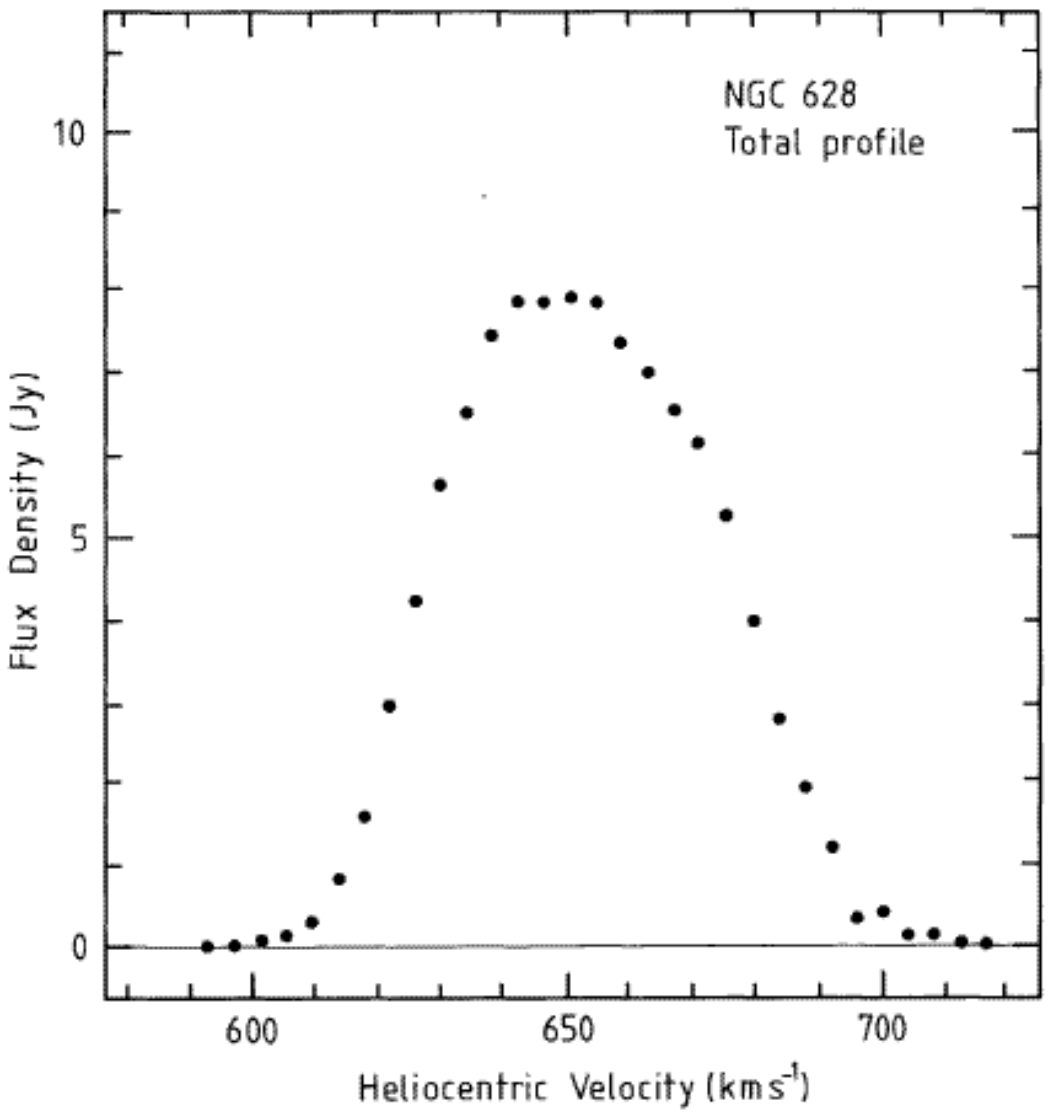


First we look at the distribution and velocity field of the HI.

The HI is much more extended than the optical image.

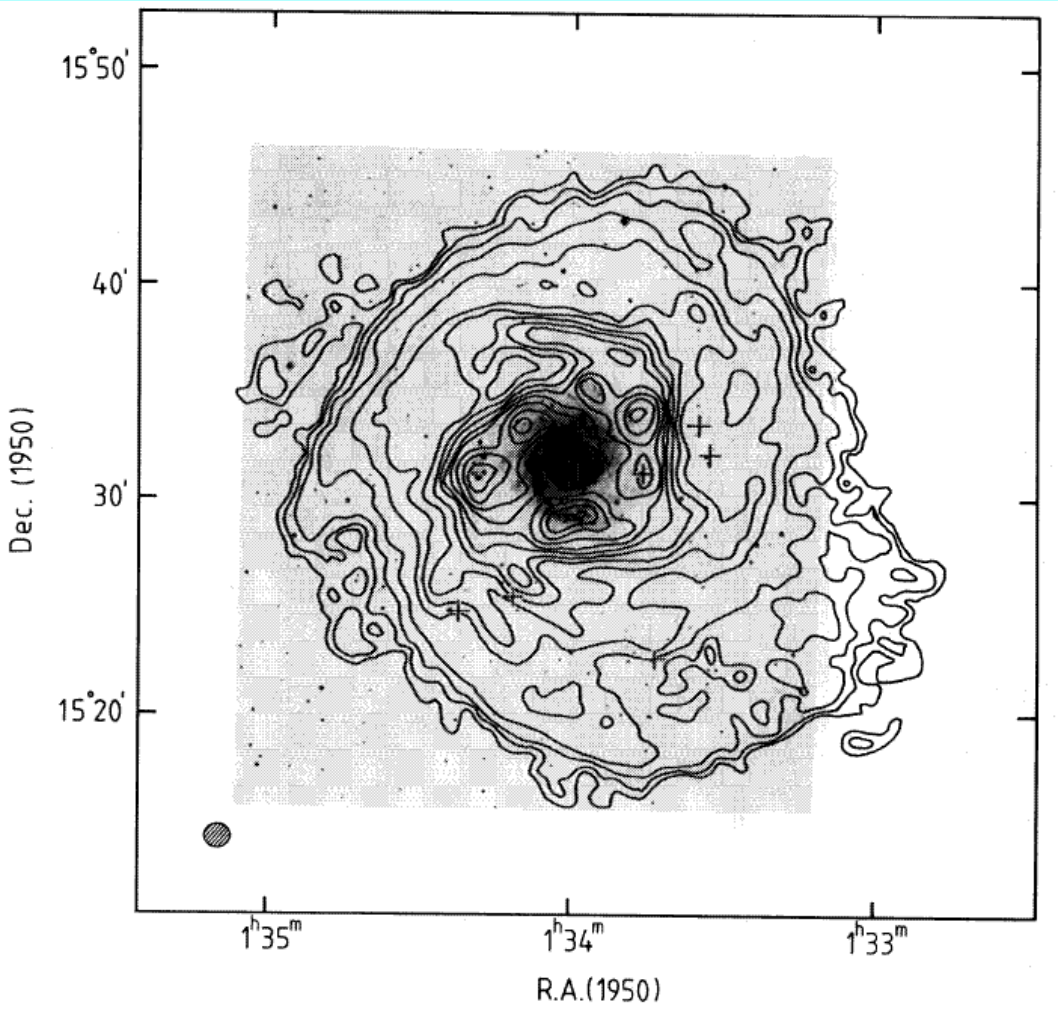


Also the spiral strcuture continues in the HI beyond the stellar disk and the optical spiral arms.

Since the disk is so close to face-on we can derive the radial distribution of the HI from simple averaging in circular annuli on the sky.

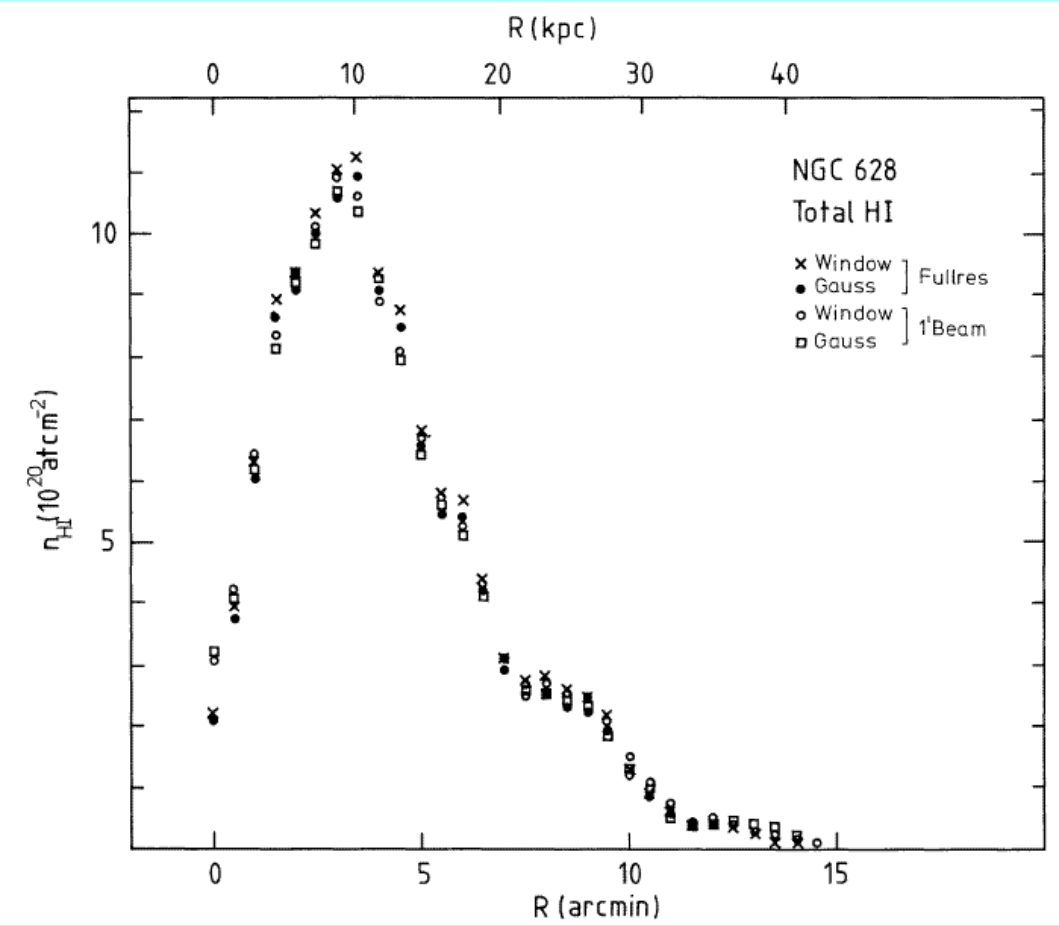


There is a feature in the profile at the edge of the stellar dsisk ($\sim$ 6 arcmin).

The velocity field looks regular in the central part, but has clear deviations in the outer part.

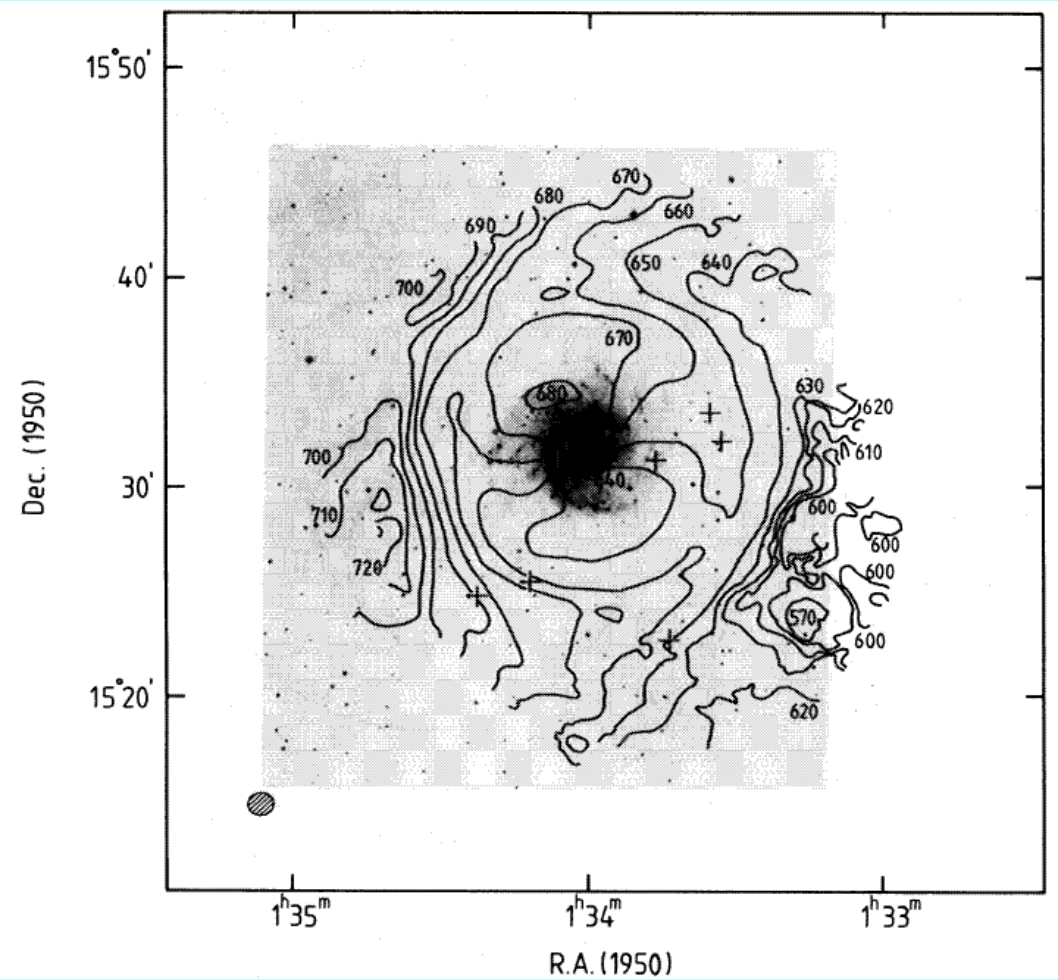


The disk is warped and the HI-plane moves actually through the plane of the sky.

At a radius of about 7 arcmin the observed velocity is about the systemic velocity.

The parameters of the tilted-ring model show this also.

At about 7 arcmin the position angle moves through a large angle and the observed rotation drops to zero and then increases again.

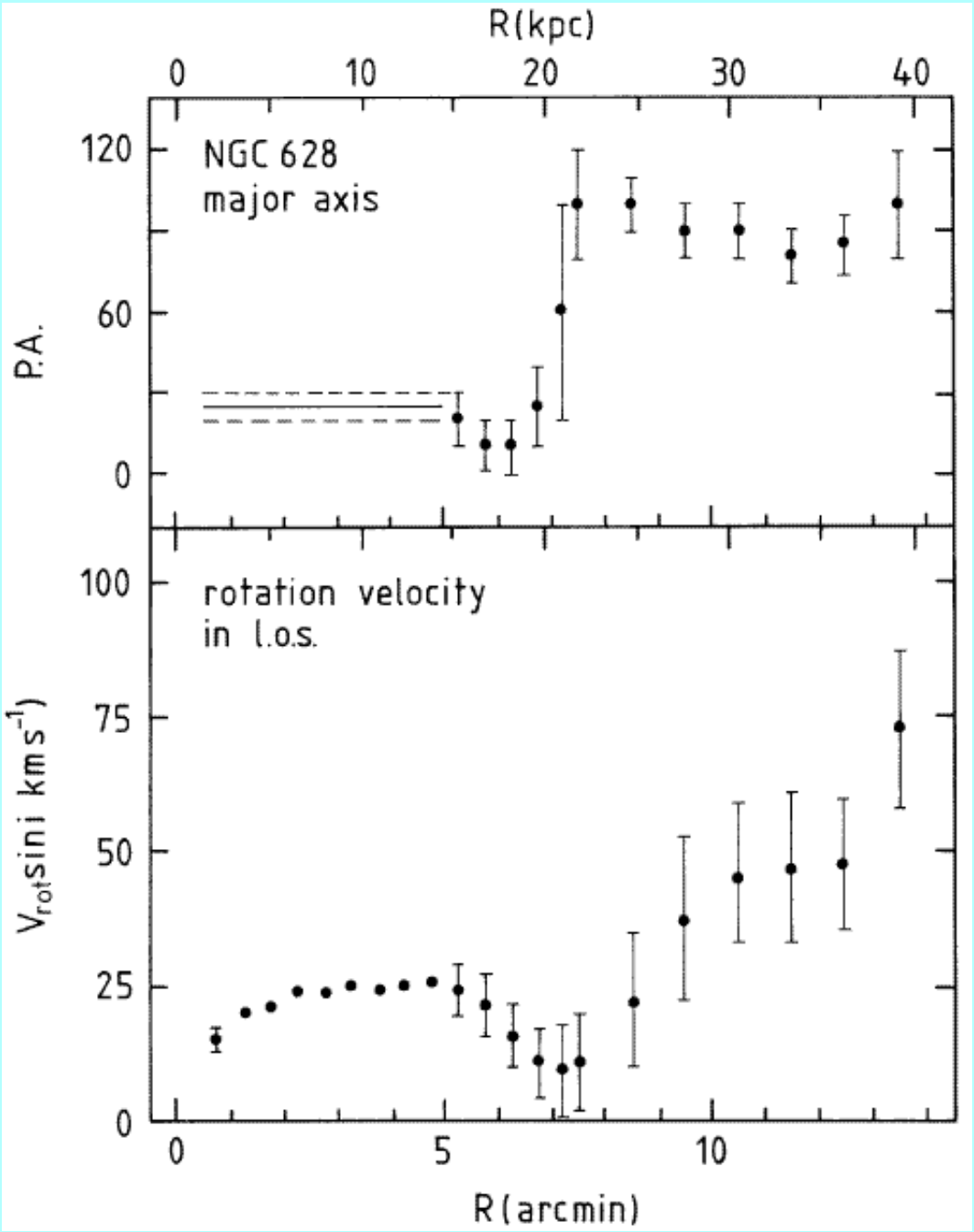

The rotation curve has an amplitude of about 25 km/s. For a galaxy of this type and absolute magnitude (according to the Tully-Fisher relation below) the rotation velocity is expected to be 200 to 250 km/s.

The inclination is then only 5 to 7°.

Over the optical part we can derive the residual velocity field when that from rotation is subtracted from the observations.

This shows no systematic pattern and has an r.m.s. value of only 3.9 km/s.

Any systematic pattern of vertical motion should be small (or mimic that of rotation) and the disk should therefore be extremely flat.

For comparison, in the solar neighborhood a vertical velocity of 4 km/s corresponds to an amplitude of only 45 pc.

The next thing we can do is determine the velocity dispersion of the HI. For this we need a face-on galaxy, because the gradient of systematic motion should be small accross a beam.

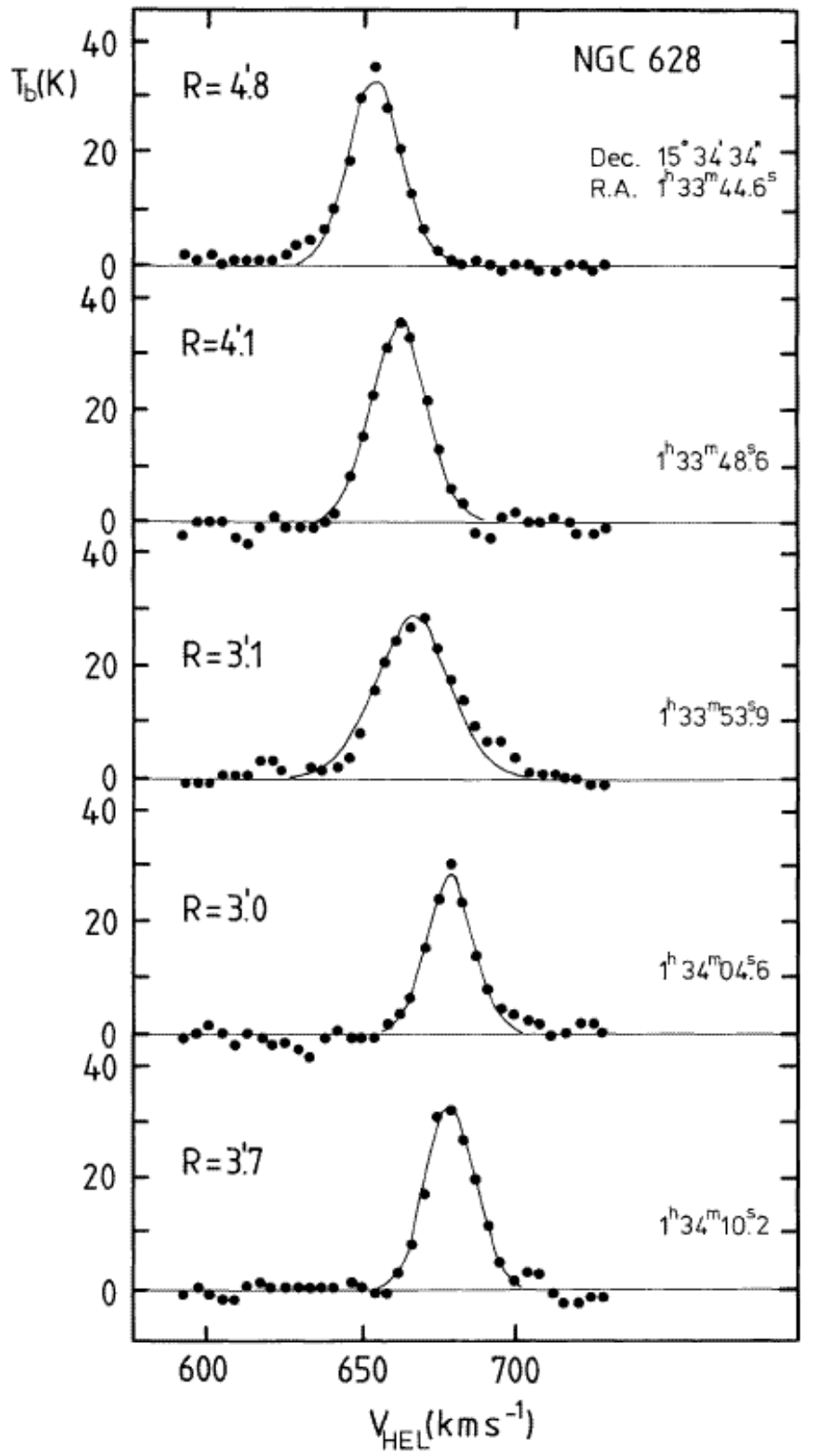
NGC 628
$T_b$(K)
R= 4'.8
Dec. 15° 34' 34"
R.A. 1h 33m 44.6s
R=4'.1
1h 33m 48s.6
R=3'.1
1h 33m 53s.9
R=3'.0
1h 34m 04s.6
R=3'.7
1h 34m 10s.2
40
20
0
600
650
700
$V_{HEL}$(km s$^{-1}$)

The HI velocity dispersion is between 7 and 10 km/s at all radii.

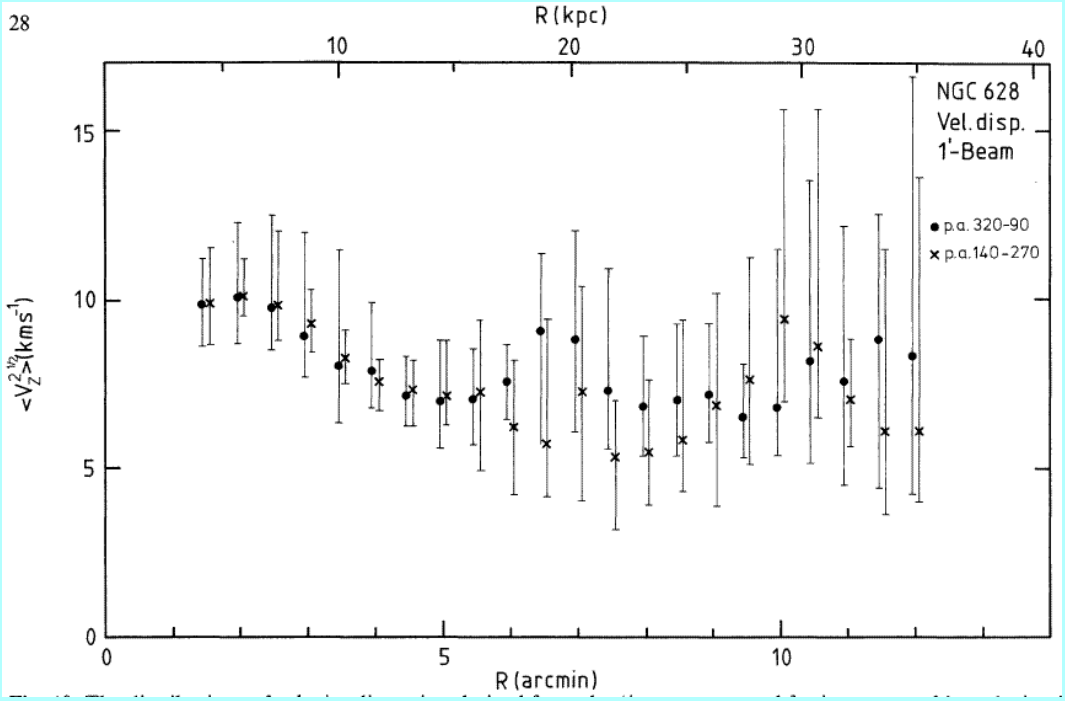


The velocity dispersion of the HI is expected to be isotropic due to cloud collisions. This is confirmed by observations of more inclined (and large angular size) galaxies.

The value of 10 km/s corresponds roughly to a kinetic temperature of $10^4$ K. This is the temperature where cooling of the interstellar medium gets very effective due to ionisation of hydrogen.

Closer analysis shows that within the optical image the velocity dispersion is systematically higher in areas of higher surface density (the spiral arms).

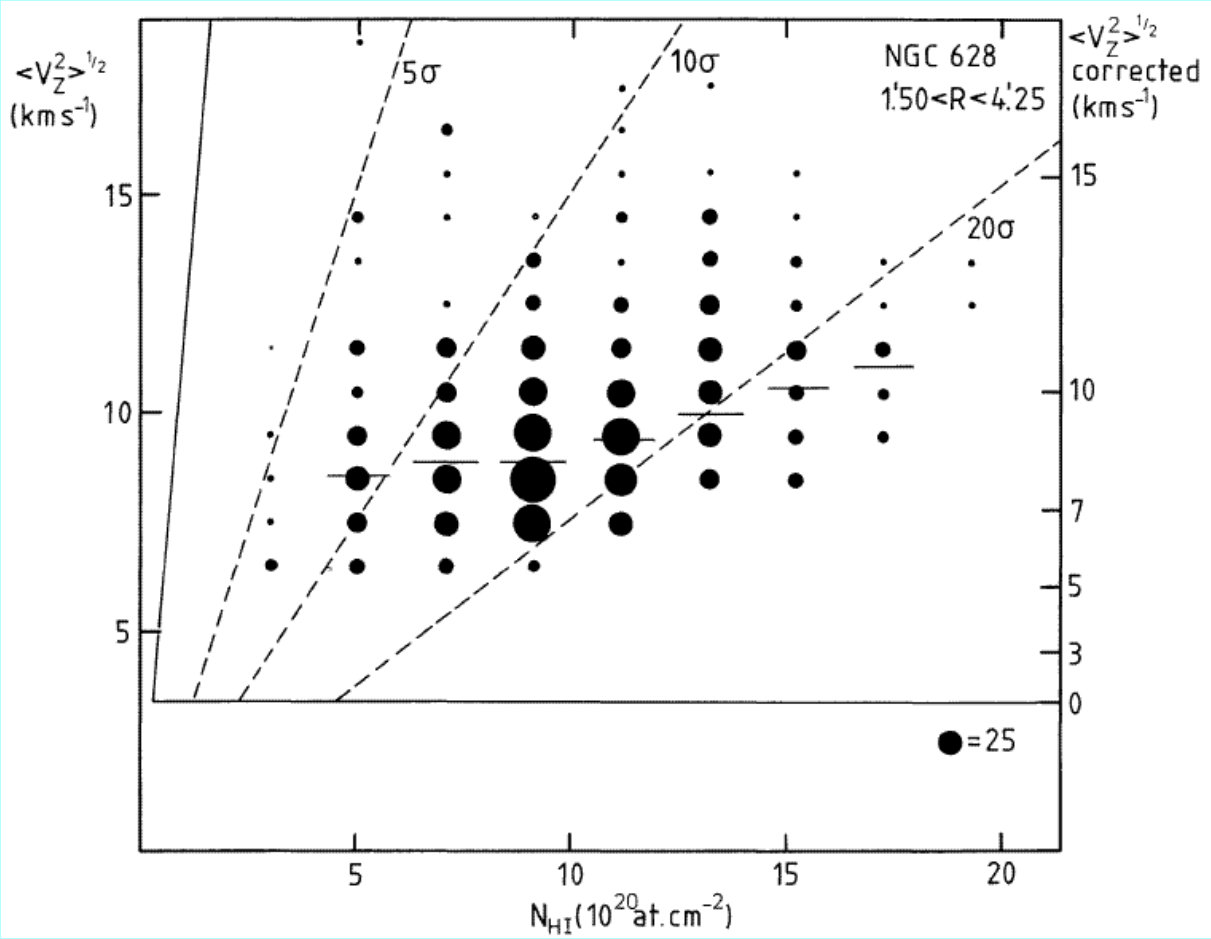


This is probably related to heating of the gas by star formation.

Now look at the edge-on galaxy NGC 891*.

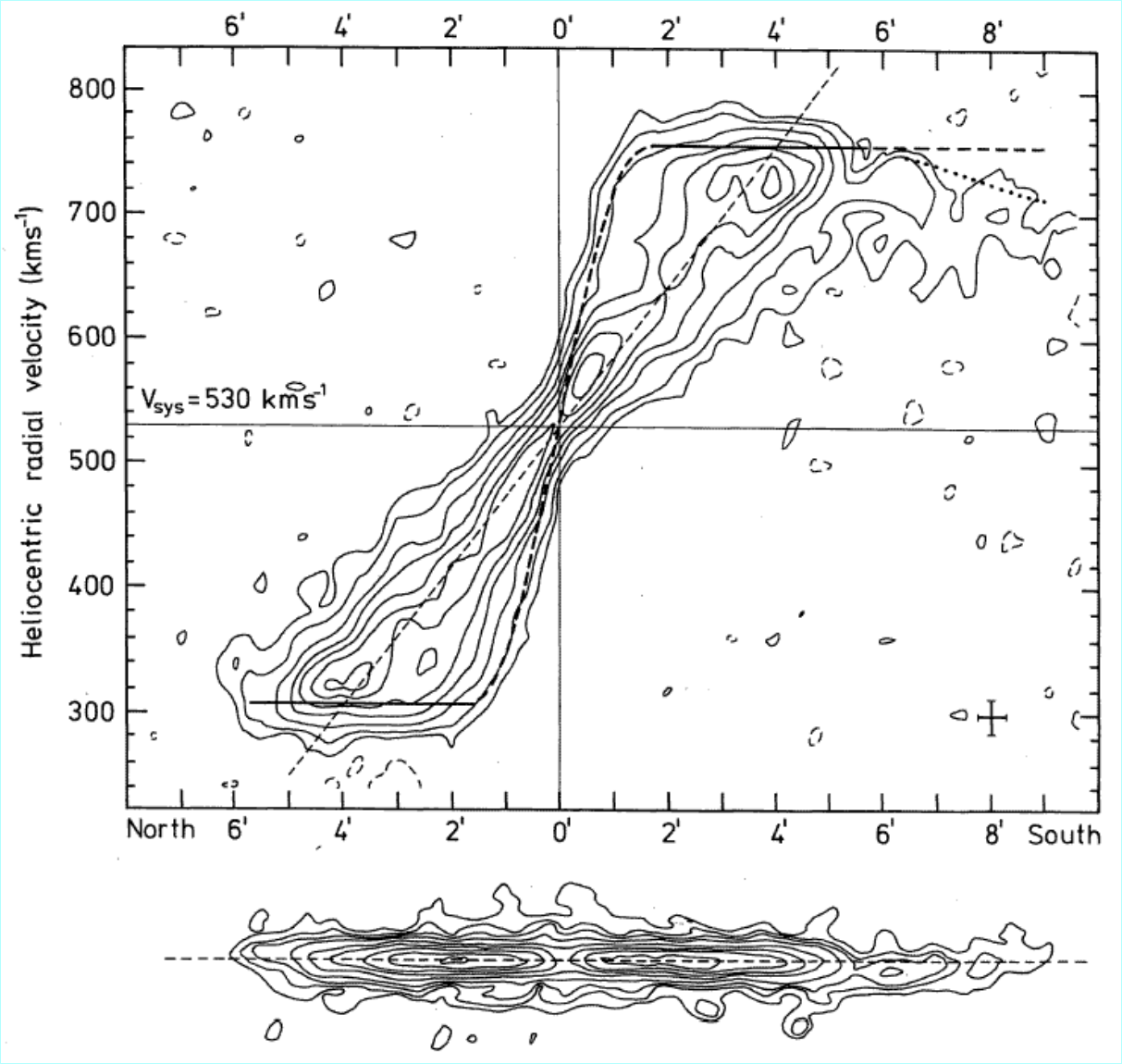


*Sancisi & Allen, A.&A. 74, 73 (1979)

The position-velocity diagram ($l, V$-diagram) now is a projection of the plane of the galaxy with only a ambiguity around the "line of nodes".

This can be seen when we draw lines of equal line of sight velocity on the plane of the galaxy.

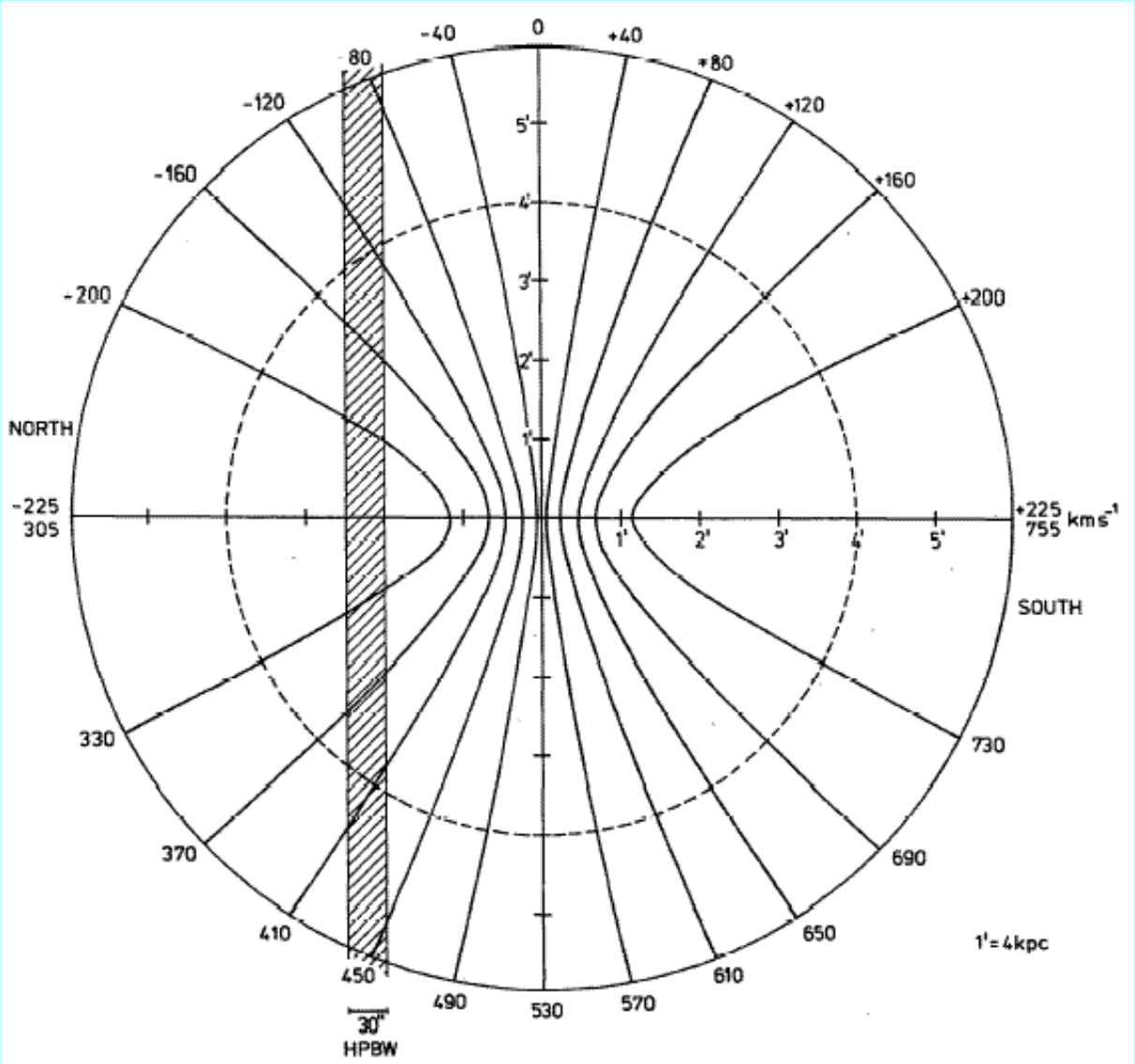

It is possible to model the $l, V$-diagram in terms of a distribution of the HI and a rotation curve.

The radial HI distribution can be estimated by "decomposing" the observed HI on the sky under the assumption of circular symmetry.

The "extreme" or "high" velocities give a first estimate of the rotation curve.

To properly model the $l, V$-diagram one needs to assume an HI velocity dispersion.

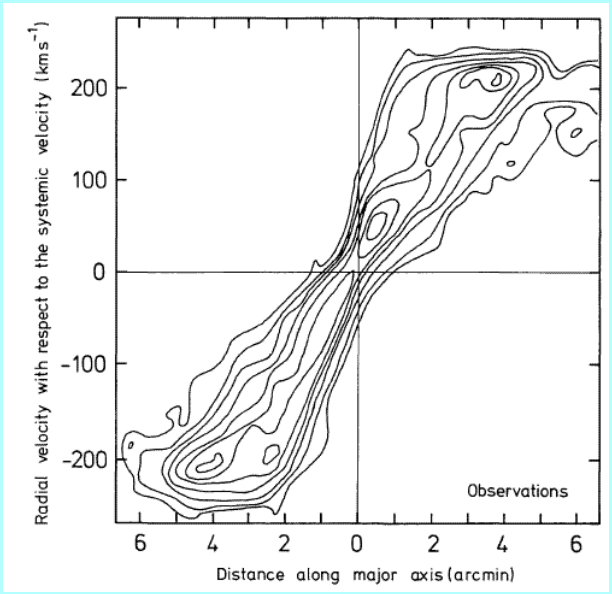


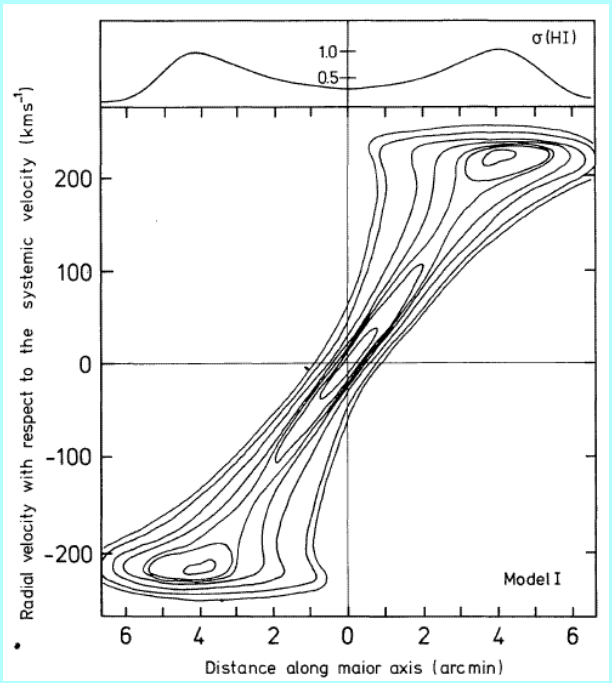

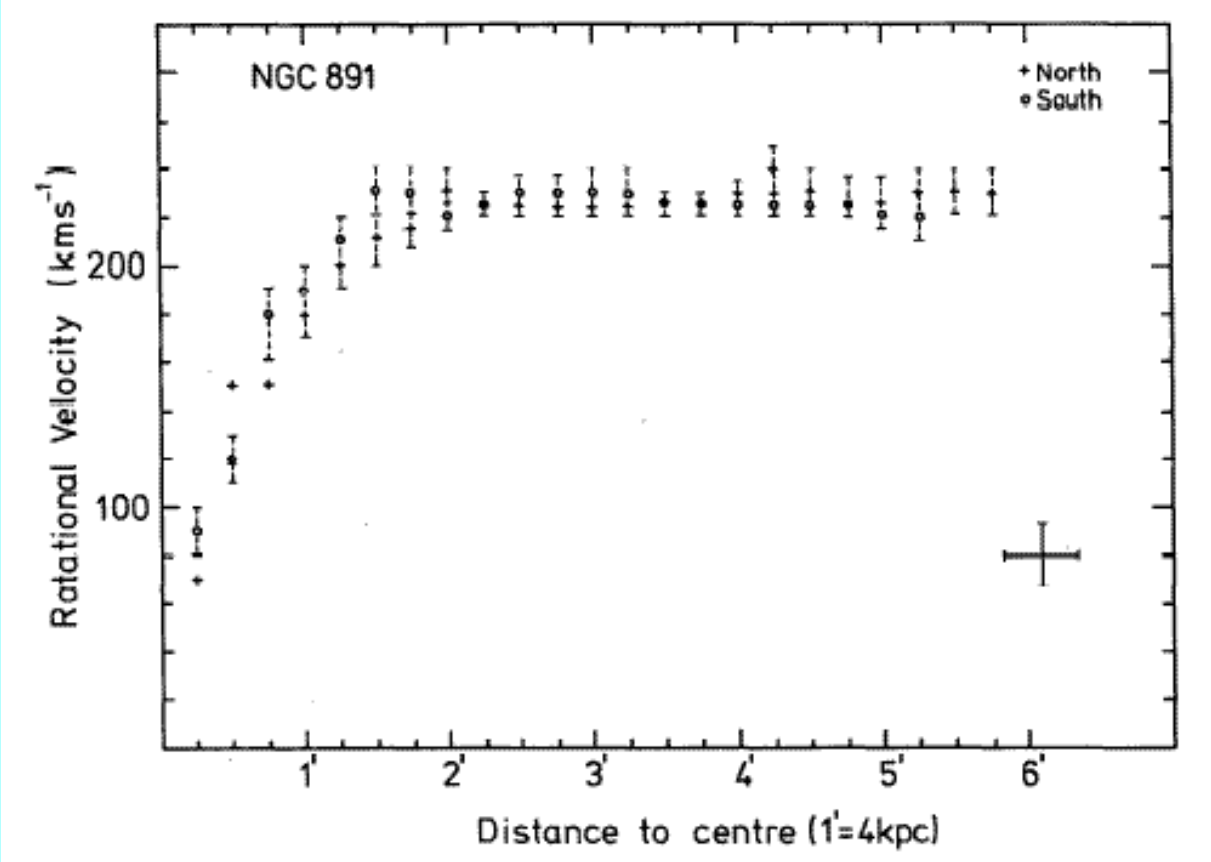


NGC 891 has not a very extended HI disk beyond the stellar disk.

Also the HI-layer appears very flat.

Other edge-on galaxies have very pronounced warps*.

*Sancisi, A.&A. 53, 159 (1976)

The most pronounced example of an HI-warp is in NGC 4013*.

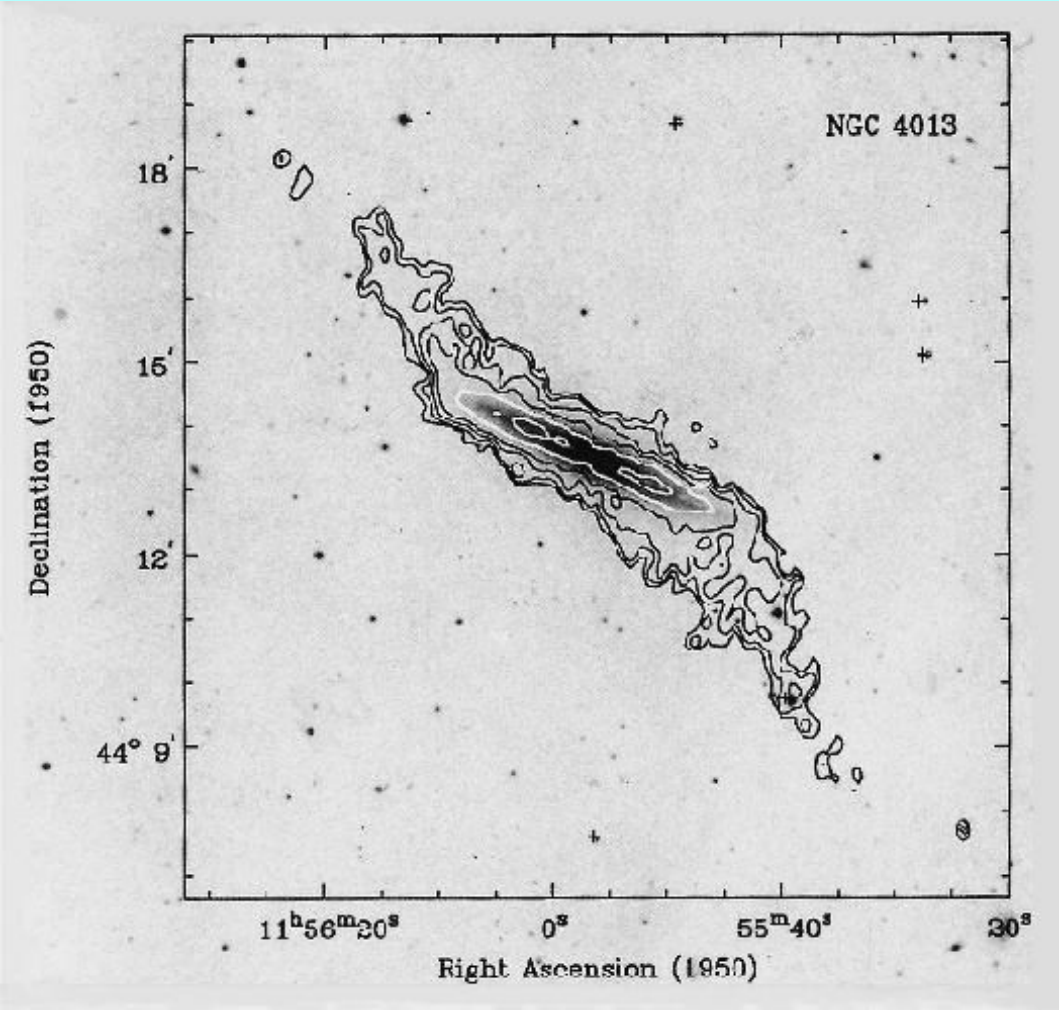


This can also be modeled with tilted-ring models.

*Bottema, Shostak & van der Kruit, Nature 328, 401 (1987), Bottema, A.&A. 295, 605 (1995) and 306, 345 (1996)

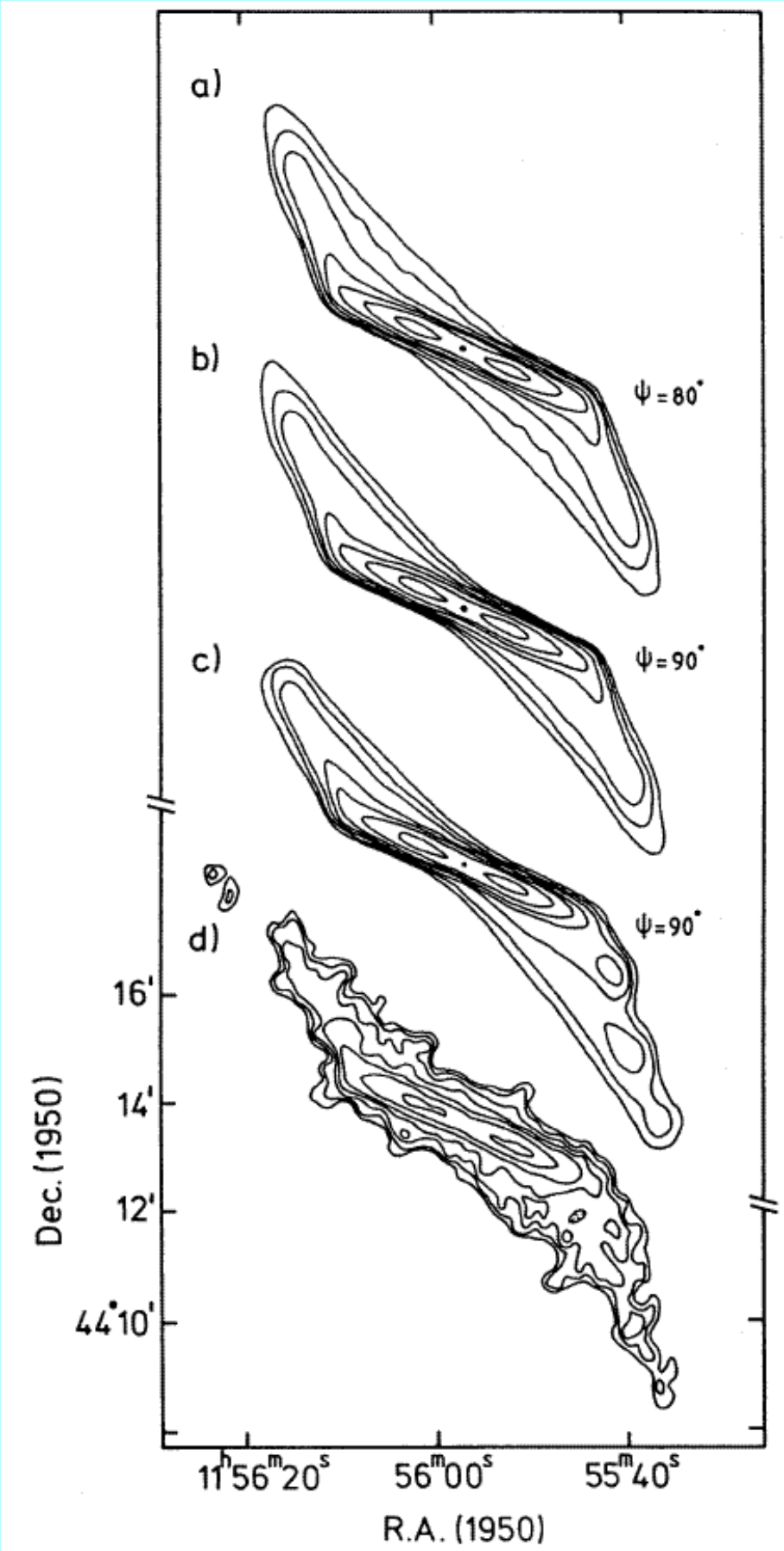
a)
b)
ψ = 80°
c)
ψ = 90°
d)
ψ = 90°
16'
14'
12'
44°10'
Dec. (1950)
11h56m20s
56m00s
55m40s
R.A. (1950)

## Stellar kinematics.

To measure stellar kinematics one needs to analyse absorption line spectra.

The assumption is that the galaxy spectrum is essentially that of a late-G to early K-giant (the "template"), shifted by a radial velocity and broadened by the velocity distribution.

The fundamental equation is

$$G(\log\lambda) = \alpha\, T(\log\lambda - \delta) \;*\; B$$

$G(\log\lambda)$ = galaxy spectrum
$T(\log\lambda)$ = template spectrum
$B$ = broadening function
$\delta$ = the radial velocity
$\langle V^2\rangle^{1/2}$ = the velocity dispersion (the second moment of $B$).

Analysis is therefore exclusively based on Fourier methods*, using:

$$\tilde{G}(k) = \gamma\, \tilde{T}(k) \cdot \tilde{B}$$

*Following the fundamental discussion by Simkin, A.&A. 31, 129 (1971)

An often used part of the spectrum is around 5000Å, where one finds the Mg b triplet and many Fe I lines.

The figure below* shows at the top galaxy exposures and below broadened spectra of template K-giants.

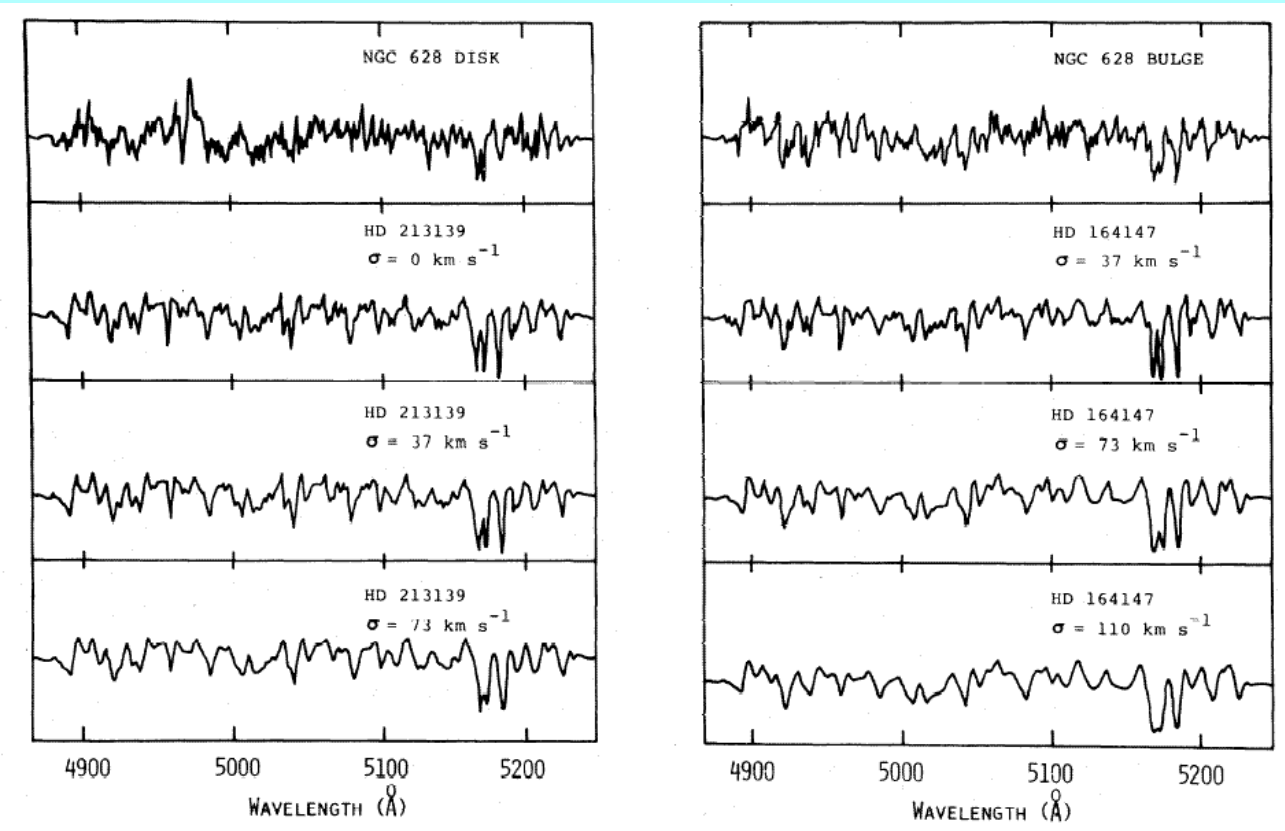


*from van der Kruit & Freeman, Ap.J. 278, 81 (1984)

There are three general methods.

Power spectrum method*.

- $\delta$ from cross-correlation peak
- $\langle V^2 \rangle^{1/2}$ from slope of power spectrum

Fourier quotient method†.

- Assume $B$ is a Gaussian
- Then $\tilde{B}$ is also a Gaussian (but complex)
- Fit a Gaussian to $\tilde{G}(k)/\tilde{T}(k)$

Cross-correlation method‡.

- $\delta$ from cross-correlation peak
- $\langle V^2 \rangle^{1/2}$ from width of cross-correlation peak

*Illingworth & Freeman, Ap. J. 188, L83 (1974)

†due to Schechter; see Sargent *et al.*, Ap.J. 212, 326 (1977)

‡Tonry & Davis, A.J. 84, 1511 (1979)

## Dynamical relations.

### a. Spiral galaxies: the Tully – Fisher relation.

For exponential disks:

$$M \propto \sigma_\circ h^2$$

$$V_{\rm max} \propto (\sigma_\circ h)^{1/2}$$

Then

$$M \propto V_{\rm max}^4 \sigma_\circ^{-1}$$

With Freeman's law and constant mass to light ratio $M/L$:

$$L \propto V_{\rm max}^4$$

This is the Tully-Fisher relation which has indeed been observed*.

In practice $V_{\rm max}$ is measured from the total width of the HI-profile, corrected for inclination, at some level defined as a percentage (20 or 50%) of the peak.

*Tully & Fisher, A.&A. 54, 661 (1977)

Aaronson & Mould* find exponents of 3.5 in B and 4.3 in H (1.6 $\mu$).

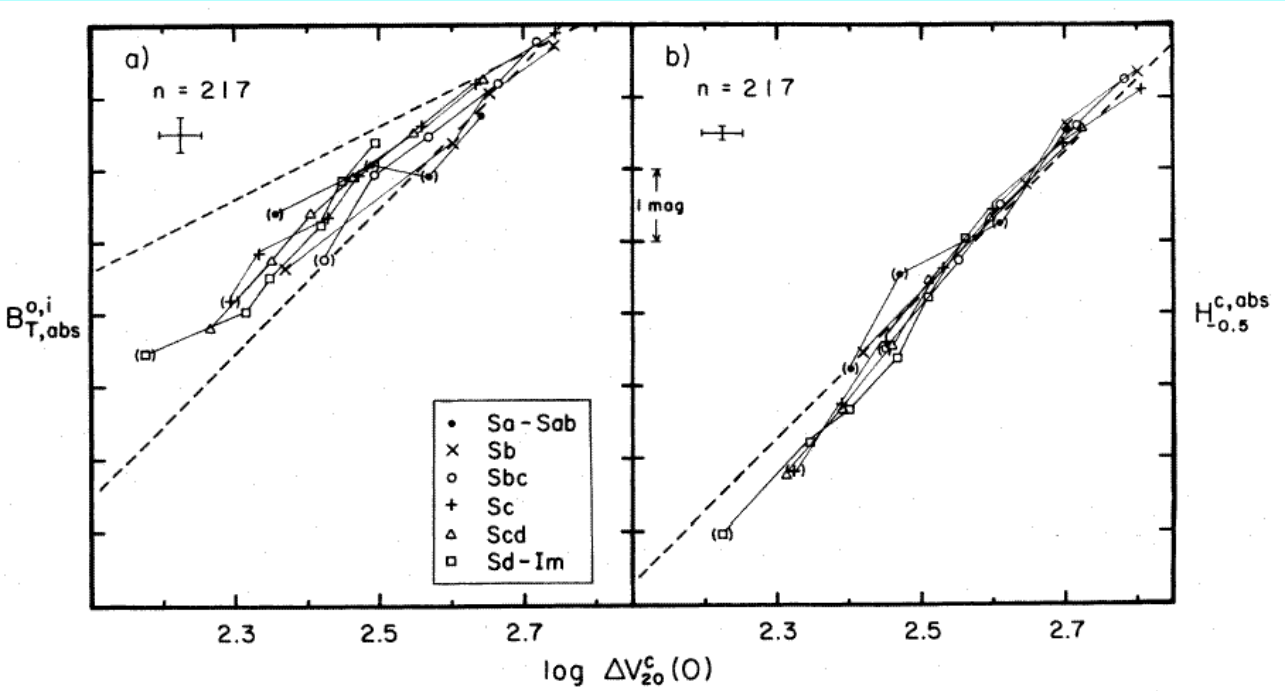


There is debate about the slope in observed relations. E.g. in the I-band Giovanelli *et al.*† find from 555 galaxies in 24 clusters a slope of $7.68 \pm 0.13$ (in magnitudes, which corresponds to $3.07 \pm 0.05$.

The data are plotted in the next figure.

*Ap.J. 265, 1 (1983)

†Ap.J. 477, L1 (1997)

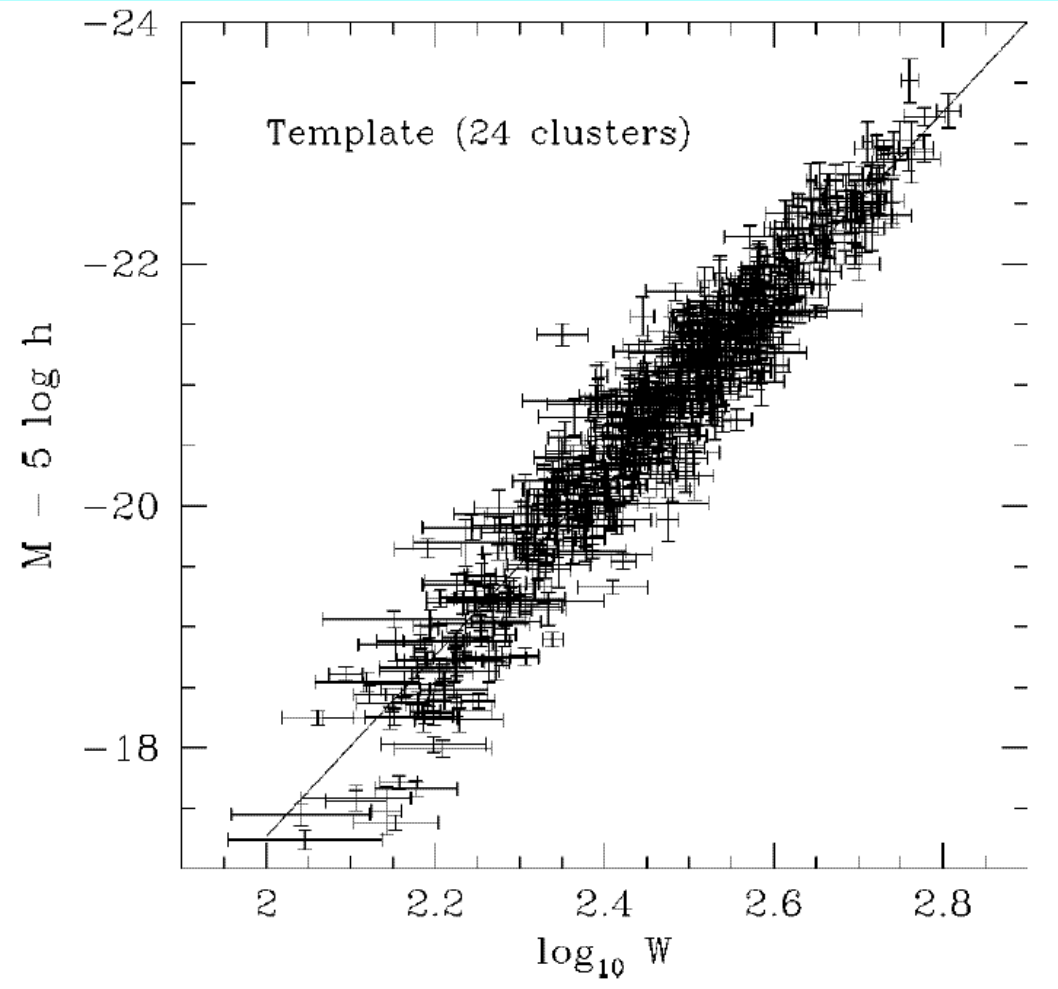


A recent study of the Ursa Major Cluster* shows that the relation is tightest in the $K'$-band and there the slope is $11.3 \pm 0.5$ (exponent $4.5 \pm 0.2$).

*Verheijen, Ph.D. thesis (1997), Ap.J. 563, 694 (2001)

## b. Elliptical galaxies: the Faber – Jackson relation and the Fundamental Plane.

We can do an equivalent thing for elliptical galaxies. The isothermal sphere has at large $R$

$$\rho(R) = \frac{\langle V^2 \rangle}{2\pi G} R^{-2}$$

The core radius is

$$r_\circ = \left( \frac{4\pi G \rho_\circ}{9\langle V^2 \rangle} \right)^{-1/2}$$

For a better description we need King-models*. For these introduce tidal radius $R_\mathrm{t}$, then

$$\langle V^2 \rangle^{1/2} \propto \rho_\circ M(R_\mathrm{t}) f\left( \frac{R_\mathrm{t}}{r_\circ} \right)$$

with $f(R_\mathrm{t}/r_\circ)$ some numerical function.
The central surface density is

$$\sigma_\circ = \rho_\circ r_\circ g\left( \frac{R_\mathrm{t}}{r_\circ} \right)$$

with $g(R_\mathrm{t}/r_\circ)$ another numerical function.

*King, A.J. 67, 471 (1962)

For ellipticals $\log(R_t/r_\circ) \approx 2.2$.

With Fish's law (constant central surface brightness) and constant $M/L$ it then follows that

$$L \propto \langle V^2 \rangle^2$$

This is what has been observed. The velocity dispersion then in practice is the one observed at the position of the center.

The scatter can even be reduced with a related three-parameter relation, that is called the Fundamental Plane.

It is a relation between some consistently defined radius (core or effective radius) $R$, the observed central velocity dispersion $\sigma$ and a consistently defined surface brightness (central or at the effective radius) $I$*:

$$R \propto \sigma^{1.4 \pm 0.15} I^{-0.9 \pm 0.1}$$

*see Kormendy & Djorgovski, Ann.Rev.Astron.Astrophys. 27, 235 (1989)

In various projections the Fundamental Plane lookes as follows.

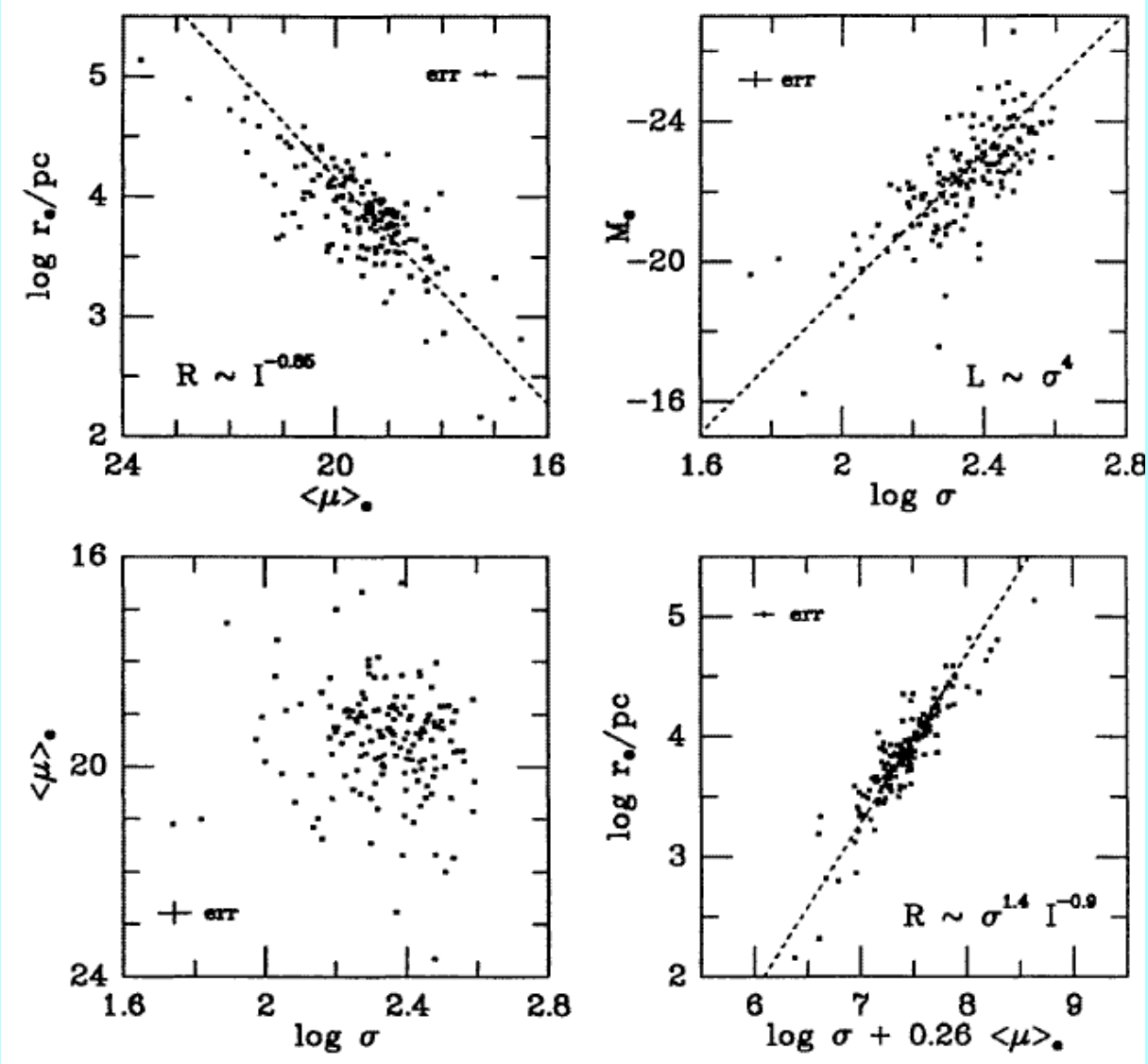


Both the Tully-Fisher relation and the Fundamental Plane are powerful means for the determination of distances.

## Distance determinations.

The most powerful methods are the following:

- Type Ia Supernovae. The peak brightness of these objects has a small intrinsic scatter.

- The Tully-Fisher relation for spiral galaxies.

- The Fundamental Plane for elliptical galaxies.

- Surface brightness fluctuations. Due to the fact that the surface brightness results from individual stars, there are statistical fluctuations. The resolution of these depends on the distance. It is applicable to ellipticals and bulges of spirals.

- Type II Supernovae. These result from massive stars and can be used through the Baade-Wesselink method.

The first three of these need calibration and the others checks with distances obtained from Cepheids.

This was done in the Key Project to measure the Hubble constant with the Hubble Space Telescope.

In this project (and related ones) direct Cepheid distances were determined for in total 31 galaxies.

The project was summarized in the final one of the 30 papers*.

The galaxies with Cepheid distances give their own distance scale. The resulting value for the Hubble constant (including only random errors) is

$$H_\circ = 75 \pm 10 \text{ km sec}^{-1}\text{Mpc}^{-1}$$

*Freedman *et al.* Ap.J. 553, 47 (2001)

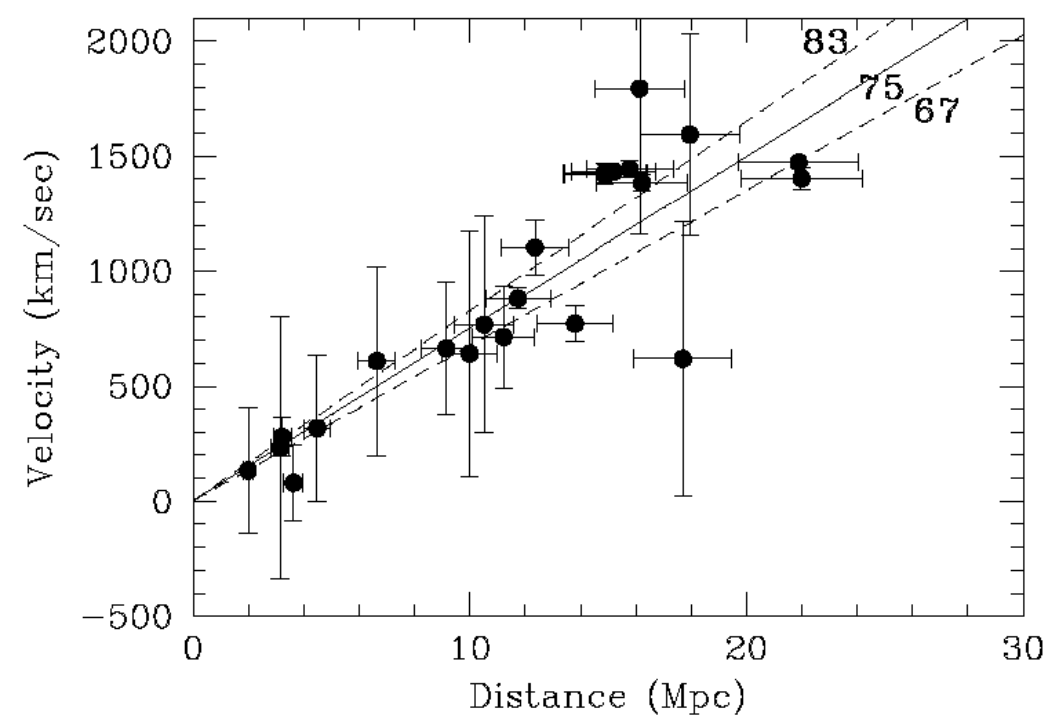


The Cepheid distances calibrate the secondary methods listed above.

It finally results (including as much as possible systematic errors) in

$$H_\circ = 72 \pm 8 \text{ km sec}^{-1}\text{Mpc}^{-1}$$